Cell Reports

Article

# XCR1+ DCs are critical for T cell-mediated immunotherapy of chronic viral infections

## Graphical abstract

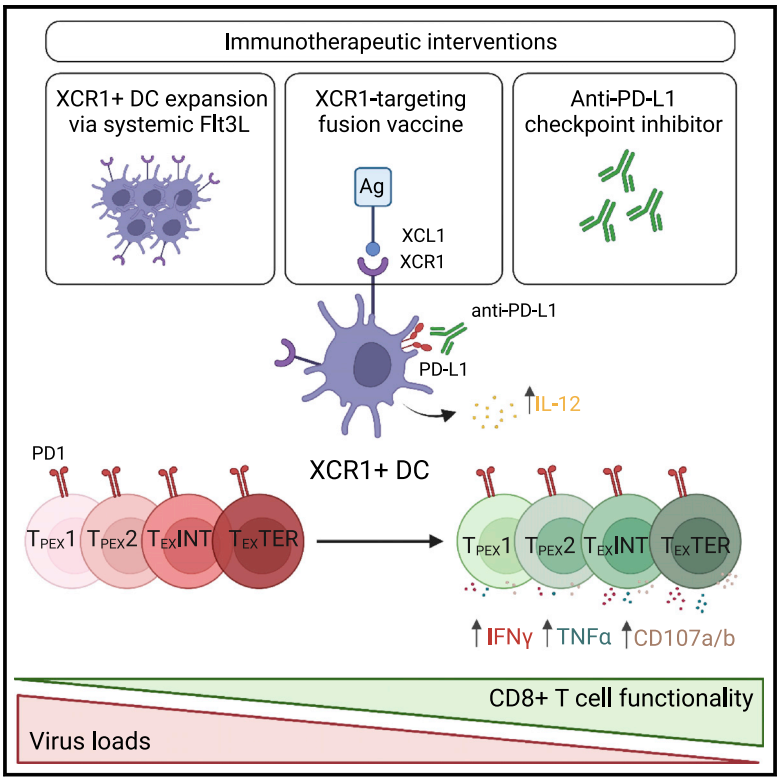


## Highlights

- XCR1+ DCs are more functional and less prone to LCMV infection than SIRPα+ DCs
- Expanding XCR1+ DCs via Flt3L or delivering XCR1-targeting Ag improve virus control
- Anti-PD-L1 treatment increases XCR1+ DC numbers and IL-12 production
- XCR1+ DCs promote $T_{EX}$ functionality but are dispensable for $T_{PEX}$ proliferation burst


## Authors

Eva Domenjo-Vila, Valentina Casella, Ryutaro Iwabuchi, ..., Gennady Bocharov, Jordi Argilaguet, Andreas Meyerhans

## Correspondence

jordi.argilaguet@irta.cat (J.A.), andreas.meyerhans@upf.edu (A.M.)



## In brief

Domenjo-Vila et al. show that XCR1+ DCs are crucial in augmenting exhausted CD8+ T cell effector functions during immunotherapeutic interventions in chronic virus infections. Increased T cell functionality leads to reduced virus loads. XCR1+ DCs should be among the preferential targets in immunotherapeutic cure strategies.


Domenjo-Vila et al., 2023, Cell Reports *42*, 112123
February 28, 2023 
https://doi.org/10.1016/j.celrep.2023.112123

CellPress

Cell Reports

CellPress
OPEN ACCESS

Article

# XCR1+ DCs are critical for T cell-mediated immunotherapy of chronic viral infections

Eva Domenjo-Vila,[1] Valentina Casella,[1] Ryutaro Iwabuchi,[2,3] Even Fossum,[4] Mireia Pedragosa,[1] Quim Castellví,[5] Paula Cebollada Rica,[1] Tsuneyasu Kaisho,[6] Kazutaka Terahara,[2] Gennady Bocharov,[7,8] Jordi Argilaguet,[1,9,*] and Andreas Meyerhans[1,10,11,*]

[1]Infection Biology Laboratory, Department of Medicine and Life Sciences (MELIS), Universitat Pompeu Fabra, Barcelona, Spain
[2]Department of Immunology, National Institute of Infectious Diseases, Tokyo, Japan
[3]Department of Life Science and Medical Bioscience, Waseda University, Tokyo, Japan
[4]Department of Immunology, Division of Laboratory Medicine, Oslo University Hospital, Oslo, Norway
[5]Department of Information and Communication Technologies, Universitat Pompeu Fabra, Barcelona, Spain
[6]Department of Immunology, Institute of Advanced Medicine, Wakayama Medical University, Wakayama, Japan
[7]Marchuk Institute of Numerical Mathematics, Russian Academy of Sciences, Moscow, Russia
[8]Sechenov First Moscow State Medical University, Moscow, Russia
[9]IRTA, Centre de Recerca en Sanitat Animal (CReSA-IRTA-UAB), Campus de la Universitat Autònoma de Barcelona, Bellaterra, Spain
[10]Institució Catalana de Recerca i Estudis Avançats (ICREA), Barcelona, Spain
[11]Lead contact
*Correspondence: jordi.argilaguet@irta.cat (J.A.), andreas.meyerhans@upf.edu (A.M.)
https://doi.org/10.1016/j.celrep.2023.112123

## SUMMARY

The contribution of cross-presenting XCR1+ dendritic cells (DCs) and SIRPα+ DCs in maintaining T cell function during exhaustion and immunotherapeutic interventions of chronic infections remains poorly characterized. Using the mouse model of chronic LCMV infection, we found that XCR1+ DCs are more resistant to infection and highly activated compared with SIRPα+ DCs. Exploiting XCR1+ DCs via Flt3L-mediated expansion or XCR1-targeted vaccination notably reinvigorates CD8+ T cells and improves virus control. Upon PD-L1 blockade, XCR1+ DCs are not required for the proliferative burst of progenitor exhausted CD8+ T ($T_{PEX}$) cells but are indispensable to sustain the functionality of exhausted CD8+ T ($T_{EX}$) cells. Combining anti-PD-L1 therapy with increased frequency of XCR1+ DCs improves functionality of $T_{PEX}$ and $T_{EX}$ subsets, while increase of SIRPα+ DCs dampened their proliferation. Together, this demonstrates that XCR1+ DCs are crucial for the success of checkpoint inhibitor-based therapies through differential activation of exhausted CD8+ T cell subsets.

## INTRODUCTION

A hallmark of chronic virus infections is the appearance of exhausted CD8+ T cells to prevent immunopathology.[1] These exhausted cells represent a distinct lineage within the CD8+ T cell population and are triggered by high antigen levels through several transcription factors including TOX.[2–5] TOX induces epigenetic modifications that result in a dysfunctional cell phenotype with impaired cytokine secretion and up-regulation of inhibitory receptors like PD-1, TIM-3, and others.[6,7] Exhausted CD8+ T cells are a heterogeneous population covering diverse differentiation states. Progenitor exhausted ($T_{PEX}$) cells are characterized by the expression of TCF1 and CXCR5 and give rise to a more effector-like yet terminally exhausted ($T_{EX}$) population displaying higher levels of inhibitory receptors including TIM-3.[8] More recently, $T_{PEX}$ and $T_{EX}$ have been further subdivided according to their accessibility to the blood circulation defined by CD69 expression. These subsets were named T progenitor exhausted 1 (CXCR5+ CD69+; $T_{PEX}1$) and 2 (CXCR5+ CD69-; $T_{PEX}2$), and T exhausted intermediate (CXCR5- CD69-; $T_{EX}$INT) and terminal (CXCR5- CD69+; $T_{EX}$TER).[9] Exhausted CD8+ T cells including $T_{PEX}$ have been detected in chronic virus infections, i.e., with lymphocytic choriomeningitis virus (LCMV)[8,10] and simian immunodeficiency virus (SIV) in animal models,[11] as well as in human infections with HIV,[12–14] HBV,[15] HCV,[16] and human cancers.[17–19]

Checkpoint inhibitors like anti-PD-1 or anti-PD-L1 antibodies that block inhibitory receptor functioning can partly reinvigorate exhausted CD8+ T cells.[20,21] They have evolved as a highly promising immunotherapeutic approach in the treatment of cancers[22,23] and are potentially advantageous against chronic infections.[24–28] Their clinical benefit is mainly mediated by $T_{PEX}$ that can massively proliferate and replenish the pool of effector-like $T_{EX}$, which restrict tumor growth and virus expansion.[8,12,29] However, to avoid therapeutic failure due to resistance to anti-PD-1/PD-L1 treatment, CD8+ T cells need to be optimally primed.[30] Mounting evidence points to cross-presenting XCR1+ dendritic cells (XCR1+ DCs) as the preferred antigen-presenting cells to choreograph and successfully prime CD8+ T cells.[31–33] These DCs are the only cell type expressing the XCR1 receptor[34] through which they sense gradients of the chemokine XCL1 produced by natural killer (NK) cells and

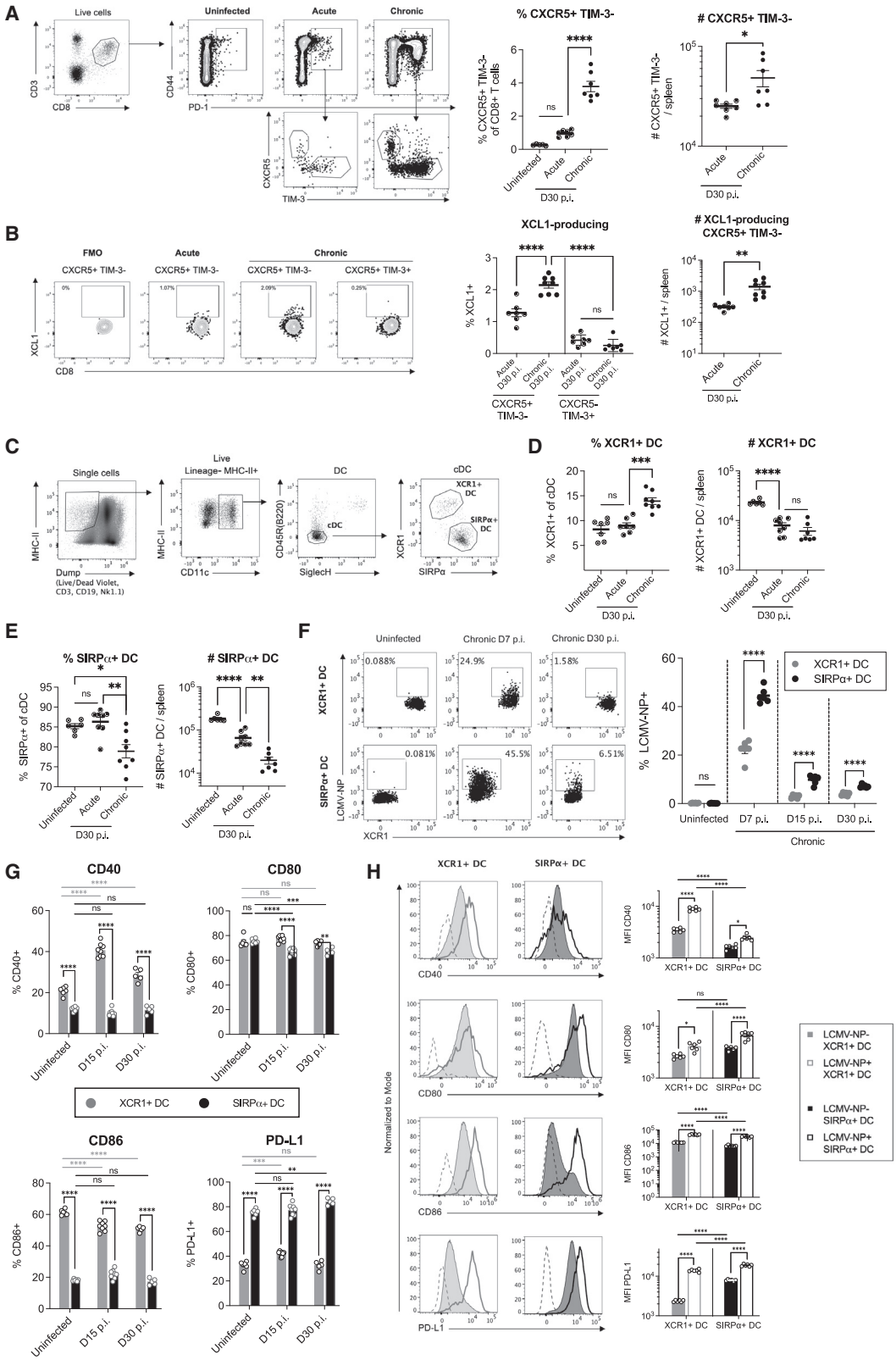


*(legend on next page)*

activated CD8+ T cells.[35–37] Homologous DC populations exist in humans[38] and rhesus macaques.[39] Cross-presenting CD103+ DCs that also express XCR1 have been identified as key elements in the control of mouse and human tumors[40,41] and they are critical for enhancing anti-tumor T cell responses upon PD-1/PD-L1 blockade.[42,43] Besides cross-presenting DCs, also SIRPα+ DCs participate in the control of tumor growth. This conventional DC population is part of the regulatory system maintaining homeostasis of the fibroblast reticular network of the spleen[44] and CD4+ T cell responses.[45] Inhibition of SIRPα+ by blocking antibodies stimulated tumor T cell recruitment and increased anti-tumor T cell responses, thus suggesting a cancer-promoting role of SIRPα+ DCs by restricting T cell access to the tumor site.[46,47] The contribution of both DC subsets in chronic virus infections has not been fully investigated.

The XCL1-XCR1 communication axis between virus-specific CD8+ $T_{PEX}$ and XCR1+ DCs is a major component in virus control during the initial phase of a chronic infection.[37] So far, it remains unclear to what extent it contributes to virus control during the established chronic infection steady-state and how it can be manipulated for host benefit. Using the mouse model of chronic LCMV infection, we show here that (1) XCR1+ DCs but not SIRPα+ DCs maintain an activation phenotype, (2) XCR1-targeting of viral antigens or expansion of XCR1+ DCs via hydrodynamic gene transfer of FMS-like tyrosine kinase 3 ligand (Flt3L) substantially improves virus control, (3) XCR1+ DCs are indispensable to promote the functionality of $T_{PEX}2$, $T_{EX}$INT and $T_{EX}$TER during anti-PD-L1 treatment but not their proliferation, and (4) increasing XCR1+ DC numbers during anti-PD-L1 treatment leads to an additional gain in the functionality of exhausted CD8+ T cells, whereas increase of PD-L1-expressing SIRPα+ DCs dampens the proliferation burst of $T_{PEX}2$ and $T_{EX}$INT. Altogether, our results revealed that XCR1+ DCs and SIRPα+ DCs affect exhausted CD8+ T cell subsets during PD-L1 immunotherapy differently and that XCR1+ DCs are a promising therapeutic target to improve virus control during a chronic viral infection.

## RESULTS

### XCR1+ DCs, but not SIRPα+ DCs, maintain an activation phenotype during chronic LCMV infection

We have previously demonstrated the importance of XCR1+ DCs in virus control during the initial phase of chronic LCMV infection.[37] Here we aimed to further investigate the role of XCR1+ DCs in the established chronic infection phase. C57BL/6J mice were chronically infected with a high dose ($2 \times 10^6$ plaque-forming units; pfu) of LCMV strain Docile ($LCMV_{Doc}$), and CD8+ T cell and DC populations were analyzed 30 days post-infection (p.i.) (Figures 1 and S1). Percentage and number of total and gp33-specific CXCR5+ TIM-3− CD8+ T cells in the spleen as well as their production of XCL1 were elevated in chronically infected mice compared with uninfected mice or mice that had recovered from an acute LCMV infection (Figures 1A–1C, S1A, and S1B). Concomitantly, chronically infected mice had a higher percentage of splenic cross-presenting DCs expressing the XCL1 receptor (XCR1+ DCs) (Figures 1D and 1E). This was the result of a marked loss of SIRPα+ DCs. Together this demonstrates the maintenance of the XCL1-XCR1 axis during the course of a chronic virus infection.

Several viruses, including LCMV, can directly infect DCs and interfere with their maturation and functioning.[48–52] However, it was recently reported that human cross-presenting DCs have an innate resistance to infections by enveloped viruses, including HIV and influenza virus, and thus preserve the host capacity to elicit an antiviral response.[53] To determine whether the marked loss of SIRPα+ DCs was linked to their increased susceptibility to LCMV infection, and whether XCR1+ DCs remain functional during chronic infection, we analyzed the percentage of intracellular LCMV nucleoprotein (LCMV-NP+) in both DC subsets and measured the expression of activation (CD40, CD80, CD86) and inhibitory (PD-L1) markers at different time points p.i. and within LCMV-NP+ and LCMV-NP− DCs (Figures 1F–1H). Throughout the different stages of infection, the percentage of SIRPα+ DCs containing LCMV-NP+ was higher than that of XCR1+ DCs (Figure 1F). XCR1+ DCs exhibited an activation phenotype with a major increase of CD40+ cells already at day 15 p.i., a steady high level of CD80 and a slight reduction of CD86 while maintaining low PD-L1 expression at all time points p.i. Conversely, SIRPα+ DCs showed an inhibitory phenotype with up to 90% positive staining for PD-L1 at day 30 p.i., displayed a low level of CD40 and CD86, and a decreasing CD80 expression as the infection progressed (Figure 1G). The expression levels of these markers at day 30 p.i. were higher in both LCMV-NP+ DC subsets (Figure 1H). Thus, the characteristics of XCR1+ and SIRPα+ DCs during LCMV infection resemble those described for other infections. The relative resistance of XCR1+ DCs to infection while maintaining their functionality makes them preferential candidates for immunotherapeutic strategies during chronic virus infection states.

**Figure 1. Phenotypic characterization of CD8+ T cells, XCR1+ DCs, and SIRPα+ DCs in chronic LCMV infection**

Mice were chronically infected with a high dose ($2 \times 10^6$ pfu) of LCMV strain Docile ($LCMV_{Doc}$), acutely infected with a low dose ($2 \times 10^2$ pfu) of LCMV or left uninfected. Splenic CD8+ T cells and DC populations were analyzed by flow cytometry.

(A) Representative gating strategy and quantification of CXCR5+ TIM-3− CD8+ T cells isolated from LCMV-infected C57BL6/J mice at day 30 p.i.

(B) Representative plots and quantification of XCL1-producing CXCR5+ TIM-3− CD8+ T cells compared with CXCR5− TIM-3+ CD8+ T cells at day 30 p.i.

(C) Representative gating strategy of splenic DCs from an LCMV-infected C57BL6/J mouse.

(D and E) Quantification of XCR1+ (D) and SIRPα+ (E) DCs at day 30 p.i.

(F) Representative plots for intracellular LCMV-NP staining and percentages of LCMV-NP+ XCR1+ and SIRPα+ DCs at the indicated time points.

(G) Percentages of CD40, CD80, CD86, and PD-L1 proteins expressed by XCR1+ and SIRPα+ DCs at the indicated time points.

(H) Representative histograms and MFI quantification for the expression of CD40, CD80, CD86, and PD-L1 on LCMV-NP+ versus LCMV-NP− XCR1+ and SIRPα+ DCs at day 30 p.i.

Data shown are the mean ± SEM from 5–10 mice per group. Statistical analysis was performed using unpaired t test (ns = not significant; *$p < 0.05$; **$p < 0.01$; ***$p < 0.001$; ****$p < 0.001$).

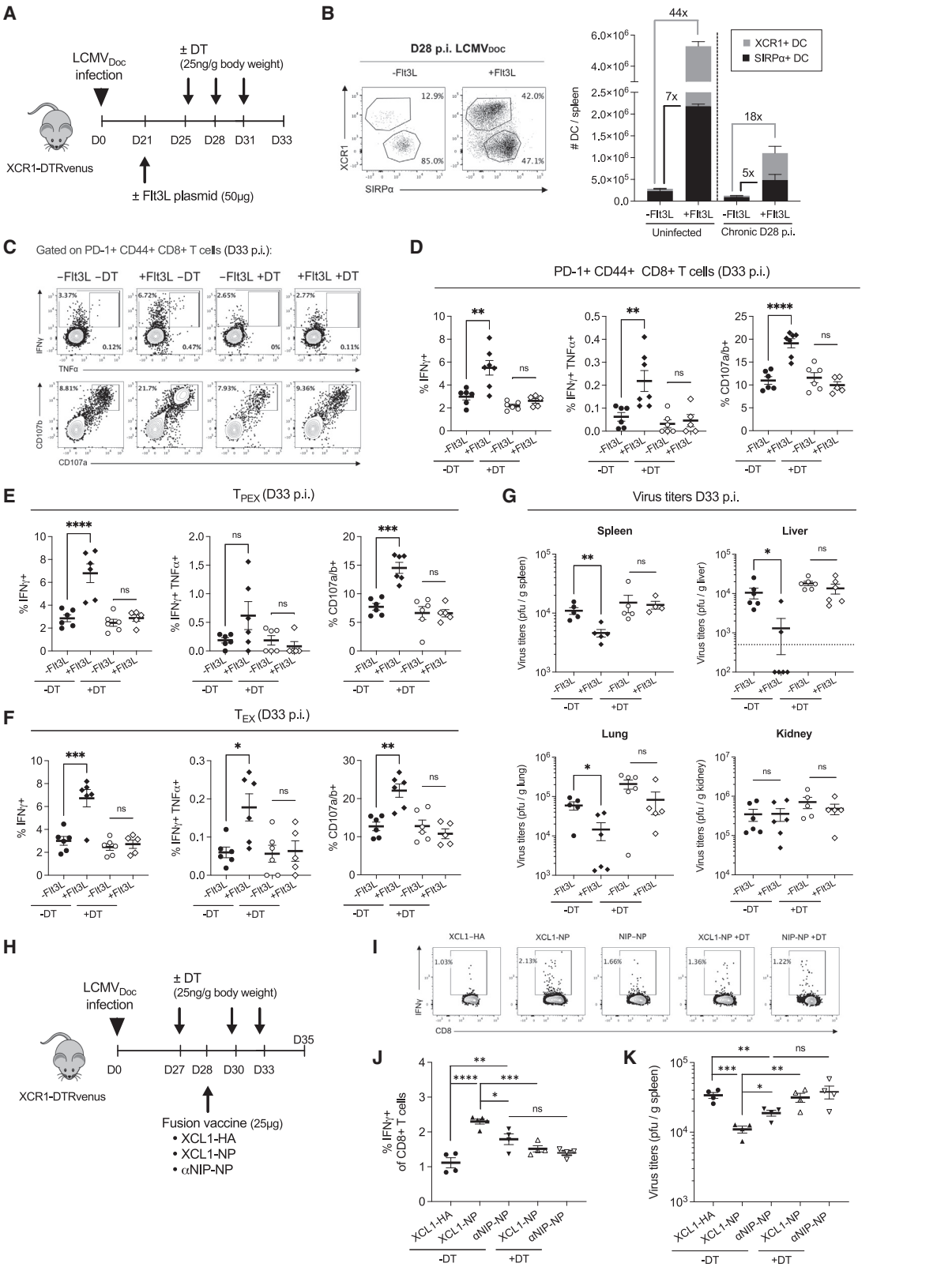


(legend on next page)

### XCR1+ DCs are critical for the therapeutic enhancement of antiviral CD8+ T cell responses

In order to assess whether XCR1+ DCs can be exploited therapeutically to improve CD8+ T cell function and restrain LCMV replication during a chronic infection, we first evaluated the effects of augmenting XCR1+ DC numbers by systemic Flt3L administration. Chronically infected and uninfected control mice were transfected *in vivo* with the pEF-BOS-Flt3L-bsr plasmid encoding the human Flt3L gene (Figure 2).[54] This procedure dramatically expanded the numbers of XCR1+ DCs and SIRPα+ DCs in uninfected (44-fold and 7-fold, respectively) and chronically infected mice (18-fold and 5-fold, respectively). The lesser increase in the latter is likely due to the previously described type-I interferon-mediated inhibition of DC maturation.[50] Considering absolute cell numbers per spleen, we observed a transient shift in the ratio of XCR1+ to SIRPα+ DCs from about 1:7 to 1:1.5, thus resulting in roughly equal absolute numbers of both cell subsets 7 days after *in vivo* transfection (Figures 2B, S2A, and S2B). DC expansion led to a functionality increase of virus-specific CD8+ T cells, pronounced in both, progenitor exhausted (CXCR5+, TIM-3−; $T_{PEX}$) and effector exhausted (CXCR5− TIM-3+; $T_{EX}$) CD8+ T cells (Figures 2C–2E, S2F, and S2G), without increasing their absolute numbers (Figures S2C–S2E). This increase in CD8+ T cell effector function resulted in virus titer reductions in spleen, liver, and lung but not in kidney (Figure 2G), an organ with limited immune cell surveillance and known to be a life-long reservoir of LCMV even after systemic clearance.[55] Further analysis at day 41 p.i. indicated that the Flt3L-mediated improvements in CD8+ T cell functionality and virus control were not sustained over time (Figures S3A–S3C). To then validate that the observed antiviral effects were mediated by XCR1+ DCs, Flt3L was administered to chronic LCMV-infected XCR1-DTRvenus mice that allow specific depletion of XCR1+ DCs by diphtheria toxin (DT) treatment (Figure 2A).[56] DT injections markedly reduced the number of XCR1+ DCs in XCR1-DTRvenus mice (Figure S2A), but not in wild-type littermates and did not affect CD8+ T cell functionality per se (Figures S3D–S3F). When XCR1+ DCs were depleted after Flt3L administration, CD8+ T cell activity remained low and virus titers remained high (Figures 2C–2G). Together, these results highlight the substantial ability of XCR1+ DCs to invigorate virus-specific exhausted CD8+ T cells and indicate their therapeutic potential during chronic virus infections.

LCMV glycoprotein (GP)-based immunogens have been shown to enhance antiviral immunity in chronic LCMV infection.[57] However, GP-specific CD8+ T cells are less exhausted and more abundant than nucleoprotein (NP)-specific CD8+ T cells.[55] To test whether XCR1+ DCs can be used as therapeutic targets even under conditions of pronounced exhaustion, fusion vaccine constructs encoding XCL1 and the LCMV nucleoprotein (XCL1-NP) were generated. These vaccines consist of dimeric XCL1-antigen fusion constructs that specifically target XCR1+ DCs and can generate protective immunity *in vivo*.[58] Chronically infected XCR1-DTRvenus mice were vaccinated with XCL1-NP. Non-targeting fusion vaccines containing a single chain variable fragment specific to the hapten NIP (αNIP-NP) and fusion vaccines encoding influenza virus hemagglutinin (XCL1-HA) were used as controls (Figure 2H). XCL1-NP induced a higher frequency of functional virus-specific CD8+ T cells than αNIP-NP with corresponding reductions in viral loads (Figures 2H–2K). This induction of functional T cells and their antiviral effect were dependent on the presence of XCR1+ DCs (Figures 2H–2K) that remained highly activated after XCL1-NP vaccination (Figure S4). Thus, XCR1+ DCs are critical for an efficient vaccine response in an established chronic infection and provide a benefit even when CD8+ T cell exhaustion is very pronounced.

### XCR1+ DCs are indispensable for increasing functionality of $T_{PEX}$2, $T_{EX}$INT, and $T_{EX}$TER during anti-PD-L1 treatment but not for their proliferation

Checkpoint inhibitors like anti-PD-L1 antibodies have been successfully used to reinvigorate exhausted CD8+ T cells.[20] To determine whether the beneficial effects derived from anti-PD-L1 immunotherapy are orchestrated by the XCL1-XCR1 communication axis, we first analyzed functional changes in $T_{PEX}$ and XCR1+ DCs in chronically infected C57BL/6J mice treated with anti-PD-L1. After treatment, more $T_{PEX}$ produced XCL1, and XCR1+ DCs were present in higher frequencies and absolute numbers in the spleen (Figures 3A and 3B). Moreover, anti-PD-L1 treatment led to a functional activation of XCR1+ DCs measured by interleukin (IL)-12(p40) and CXCL-9 cytokine production, effector cytokines known to promote T cell activation and recruitment (Figures 3C and 3D).[59–61] It also significantly increased the frequency of interferon gamma (IFNγ)+, IFNγ+ tumor necrosis factor alpha (TNFα)+, and CD107a/b + virus-specific CD8+ T cells (Figures 3E and 3F). To then test whether CXCL-9 or IL-12 signaling influenced exhausted CD8+ T cells, we neutralized these cytokines in anti-PD-L1-treated mice (Figure 3E). Neutralization of CXCL-9 did not interfere with the anti-PD-L1-mediated effects, but neutralization of IL-12 significantly reduced the functionality of PD-1+ CD44+ CD8+ T cells (Figure 3F). Of note, the functionality of $T_{PEX}$ cells remained unaltered

**Figure 2. XCR1+ DCs are critical for enhancing antiviral CD8+ T cell immunity in chronic infections**

(A) Schematic representation of Flt3L and DT treatment regimens in chronic LCMV-infected XCR1-DTRvenus mice.

(B) Representative plots and quantification of XCR1+ (gray) and SIRPα+ (black) DCs in the spleen from uninfected or chronically infected mice 7 days after transfection with empty vector pEF-BOS-bsr plasmid (-Flt3L) or pEF-BOS-Flt3L-bsr plasmid (+Flt3L). Data shown are the mean ± SEM, and the fold change over empty vector pEF-BOS-bsr plasmid transfection (n = 2–6 mice).

(C–G) Representative plots and frequency of $GP_{33-41}$-specific IFNγ-producing, IFNγ- and TNFα-producing, and CD107a/b+ splenic PD-1+ CD44+ CD8+ T cells (C and D), $T_{PEX}$ (E), and $T_{EX}$ (F) cells, and viral loads in spleens, livers, lungs, and kidneys (G) from Flt3L-treated (+Flt3L) or untreated (−Flt3L) mice at 33 days p.i.

(H) Schematic representation of fusion vaccine and DT treatment regimens in chronically infected XCR1-DTRvenus mice.

(I–K) Representative plots and quantification of $NP_{396-404}$-specific IFNγ-producing CD8+ T cells (I and J) and viral loads (K) in spleen from DT-treated or untreated vaccinated mice at day 35 p.i.

Data shown are the mean ± SEM from 4–6 mice per group. Statistical analysis was performed using one-way ANOVA with Tukey's multiple comparisons (ns = not significant; *p < 0.05; **p < 0.01; ***p < 0.001; ****p < 0.0001).

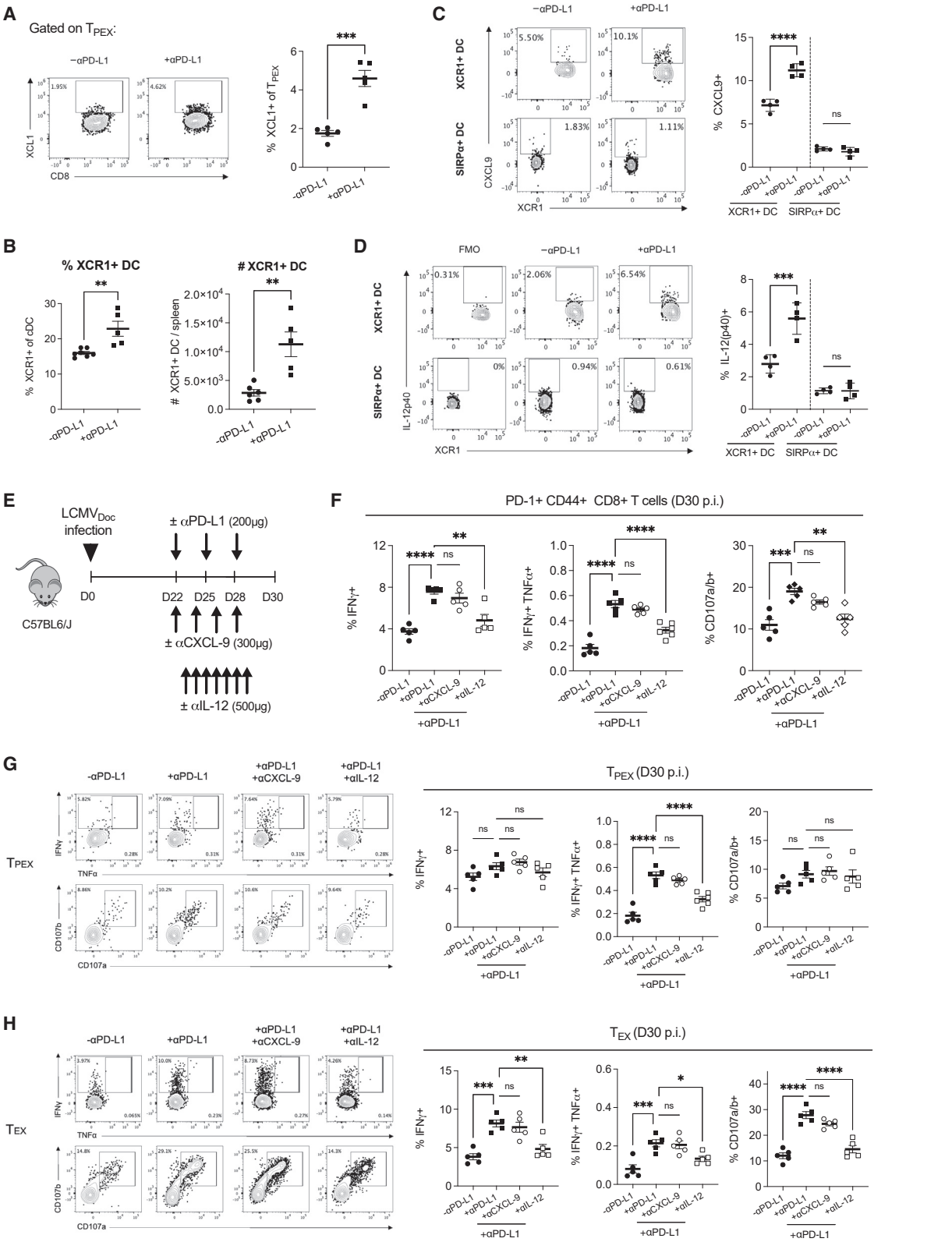


*(legend on next page)*

among conditions, and changes were mainly observed for $T_{EX}$ cells (Figures 3G and 3H).

To further investigate to which degree XCR1+ DCs participate in the immunotherapeutic effect elicited by anti-PD-L1 blockade, we compared the anti-PD-L1-induced CD8+ T cell responses and viral titers in the presence or absence of XCR1+ DCs in chronically infected XCR1-DTRvenus mice (Figure 4A). The increase in the frequency of IFNγ+ and IFNγ+ TNFα+ virus-specific CD8+ T cells and reduction in virus loads (Figures 4B and 4C) were both dependent on the presence of XCR1+ DCs, thus demonstrating the crucial contribution of XCR1+ DCs in anti-PD-L1 immunotherapy.

To analyze the dependence of progenitor exhausted $T_{PEX}$ and terminally exhausted $T_{EX}$ populations on XCR1+ DCs during anti-PD-L1 blockade in chronic infection, we quantified their proliferation by Ki67 expression and functionality by IFNγ and TNFα production. Anti-PD-L1 treatment induced proliferation of gp33-specific $T_{PEX}$ leading to an increase in absolute numbers. This increase was not altered by XCR1+ DC depletion (Figures 4D and 4E). We then performed the same analysis using the newly established classification of exhausted CD8+ T cell subsets: T progenitor exhausted 1 (CXCR5+ CD69+; $T_{PEX}1$) and 2 (CXCR5+ CD69-; $T_{PEX}2$), and T exhausted intermediate (CXCR5− CD69−; $T_{EX}$INT) and terminal (CXCR5− CD69+; $T_{EX}$TER).[9] Anti-PD-L1 induced the proliferation of $T_{PEX}2$ and $T_{EX}$INT independently from XCR1+ DC (Figures 4F and S5A), and changed the frequencies of the four subsets among gp33-specific exhausted CD8+ T cells, favoring $T_{PEX}2$ and $T_{EX}$INT subsets over $T_{EX}$TER (Figures 4G and S5B). Interestingly, these anti-PD-L1-mediated changes in relative frequencies were not observed when XCR1+ DCs were depleted. Without XCR1+ DCs, the subset distribution resembled that of untreated controls with $T_{EX}$TER being a predominant population (Figure 4G). Regarding functionality, anti-PD-L1 treatment increased the frequencies of IFNγ+ and IFNγ+ TNFα+ $T_{EX}$ cell subsets ($T_{EX}$INT and $T_{EX}$TER) and $T_{PEX}2$. This functionality increase was strictly dependent on XCR1+ DCs (Figures 4H–4K, S5C, and S5D). Taken together, these results demonstrate that XCR1+ DCs are indispensable to promote $T_{EX}$ antiviral activity during anti-PD-L1 immunotherapy but are not important for the proliferation burst of $T_{PEX}$ stem-like progenitors.

## XCR1+ DCs reduce terminal differentiation of exhausted CD8+ T cells during combination therapy

To first examine whether anti-PD-L1 immunotherapy could be further improved by targeting viral antigens to XCR1+ DCs, we treated chronic LCMV-infected C57BL/6J mice with anti-PD-L1, and simultaneously vaccinated them with XCL1-NP or the negative control XCL1-HA (Figure 5A). The massive increase of virus-specific IFNγ-producing CD8+ T cells and subsequent virus reduction upon anti-PD-L1 treatment could not be further enhanced by XCL1-NP (Figure 5B). In all cases, virus load reductions corresponded inversely to the CD8+ T cell responses (Figure 5C). Heightened CD8+ T cell function was observed in $T_{EX}$ cells, but not in $T_{PEX}$ cells (Figures 5D and 5E). Similarly, increased T cell functionality was observed in the $T_{EX}$INT, $T_{EX}$TER and $T_{PEX}2$ populations, but not the $T_{PEX}1$ population (Figure 5F). Together this demonstrated that anti-PD-L1 treatment alone or single XCL1-NP vaccination led to similar immunotherapeutic effects in chronic virus infection.

We next tested whether the lack of immune enhancement by the combination of anti-PD-L1 and XCL1-NP vaccines could be explained by insufficient numbers of XCR1+ DCs. For this we combined anti-PD-L1 and Flt3L treatments in chronic LCMV-infected XCR1-DTRvenus mice and evaluated the contribution of XCR1+ DCs by DT-mediated depletion (Figure 6A). Coupling anti-PD-L1 therapy with XCR1+ DC expansion led to a significant increase in the frequency of IFNγ-producing CD8+ T cells compared with anti-PD-L1 treatment alone (Figure 6B). However, there was no reduction in virus loads (Figure 6C). Depletion of XCR1+ DCs by DT abolished the frequency increase of IFNγ+ CD8+ T cells and resulted in increased viral loads that were highest in Flt3L-transfected mice (Figure 6C). To understand the discrepancy between the increased frequency of effector CD8+ T cells and lack of improved virus control, we analyzed the different exhausted CD8+ T cell subsets individually. Combination treatment of anti-PD-L1 and Flt3L resulted in higher frequencies of IFNγ-producing $T_{PEX}$ and $T_{EX}$ cells (Figures 6D and 6E), particularly in the $T_{PEX}1$ and $T_{EX}$TER subpopulations that almost doubled relative to anti-PD-L1 treatment alone (Figures 6F and S6A). However, this frequency increase was not a consequence of increased proliferation. Rather, Flt3L partially abrogated anti-PD-L1-induced $T_{PEX}$ proliferation and resulted in reduced absolute numbers of both $T_{PEX}$ and $T_{EX}$ without altering the relative frequency of the exhausted CD8+ T cell subsets (Figures 6H–6J, S6B, and S6C). Upon XCR1+ DC depletion, Flt3L treatment led to accumulation of the $T_{EX}$TER subset over $T_{EX}$INT. Thus, XCR1+ DCs are not only critical for the functional enhancement of exhausted CD8+ T cell subsets (see Figure 4) but also reduce their terminal differentiation. In contrast, SIRPα+ DC expansion upon Flt3L administration in the absence of XCR1+ DCs contributed to terminal differentiation (Figure 6J). These two features of the DC subsets, namely to promote or prevent accelerated terminal exhaustion, have been very recently demonstrated and are consistent with our observations.[62,63]

**Figure 3. Anti-PD-L1 treatment enforces the XCL1-XCR1 communication axis**

(A–D) Chronically LCMV-infected mice were treated with anti-PD-L1 antibody (+αPD-L1) at days 22, 25, and 28 p.i. or left untreated (−αPD-L1) and killed at day 30 p.i. Representative plots and quantification of XCL1-producing $T_{PEX}$ (A), XCR1+ DCs (B), IL-12(p40)-producing (C), and CXCL-9-producing (D) XCR1+ and SIRPα+ DCs.

(E) Schematic representation of anti-PD-L1, anti-CXCL-9, and anti-IL-12 treatment regimens in chronic LCMV-infected C57BL6/J mice.

(F) Spleens were harvested to quantify the percentage of $GP_{33-41}$-specific IFNγ-producing and CD107a/b+ PD-1+ CD44+ CD8+ T cells.

(G–I) Representative plots and of $GP_{33-41}$-specific IFNγ- and TNFα-producing and CD107a/b + $T_{PEX}$ (H) and $T_{EX}$ (I) cells are shown.

Data shown are the mean ± SEM from 4–6 mice per group. Statistical analysis was performed using unpaired t test or one-way ANOVA with Tukey's multiple comparisons (ns = not significant; *p < 0.05; **p < 0.01; ***p < 0.001; ****p < 0.0001).

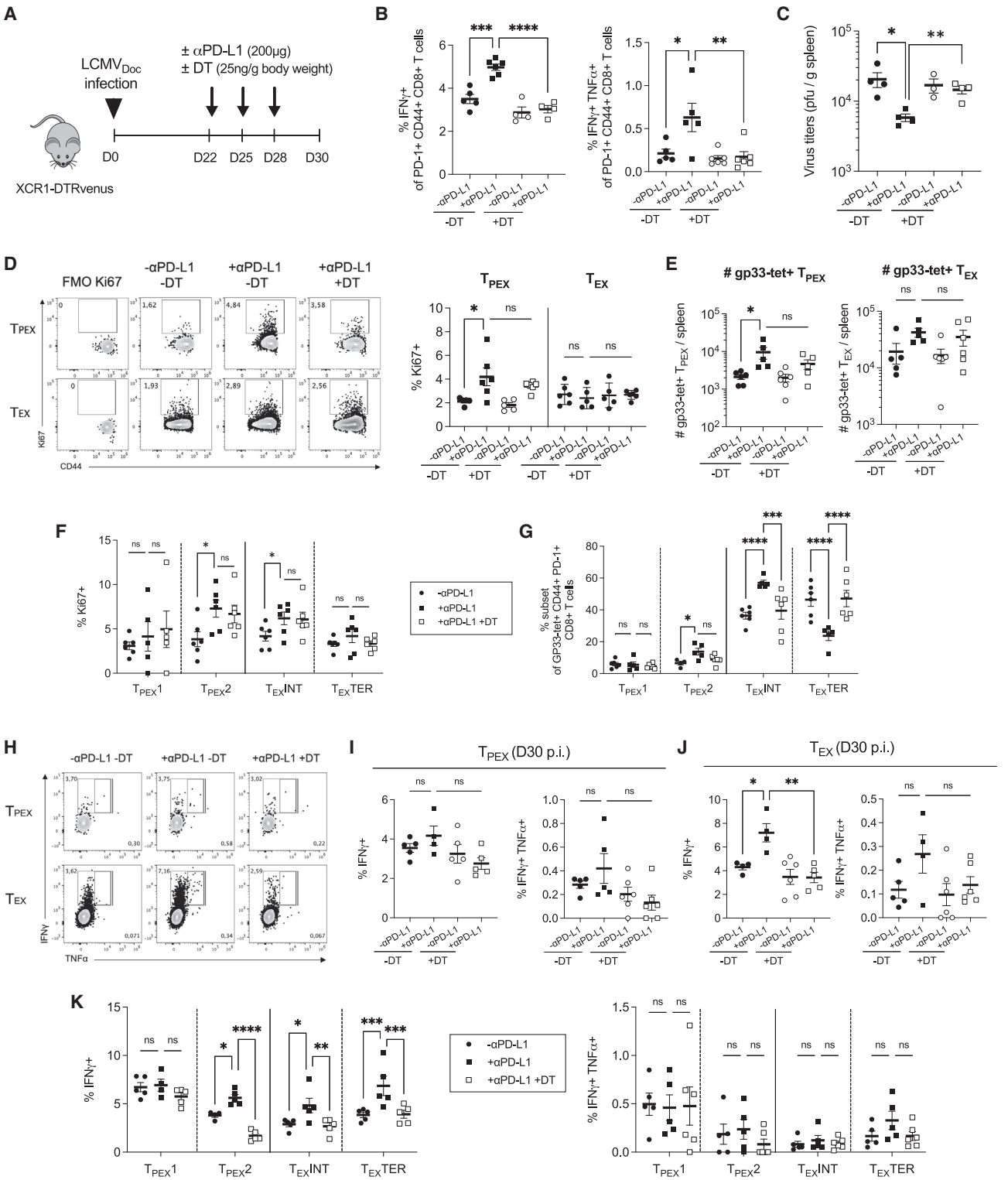


**Figure 4. XCR1+ DCs are essential to maintain functionality of effector $T_{EX}$ subsets during anti-PD-L1 treatment**

(A) Schematic representation of anti-PD-L1 and DT treatment regimens in chronic LCMV-infected XCR1-DTRvenus mice. Chronic infected anti-PD-L1 treated (+αPD-L1) or untreated (−αPD-L1) mice were killed at day 30 p.i. and spleens were harvested for analysis.

(B and C) Percentage of $GP_{33-41}$-specific IFNγ-producing and IFNγ- and TNFα-producing PD-1+ CD44+ CD8+ T cells (B) and viral loads (C).

(D and E) Representative plots and quantification of Ki-67+ proliferating gp33-tet+ $T_{PEX}$ and $T_{EX}$ (D) and their absolute numbers in spleen (E).

*(legend continued on next page)*

## DISCUSSION

In the present study we demonstrate the role of XCR1+ DCs in maintaining the chronic state of a virus infection. Chronic infections are characterized by a dynamic equilibrium of virus expansion and CD8+ T cell-mediated control. Perturbing this equilibrium by (1) targeting viral antigens to XCR1+ DCs, (2) blocking inhibitory checkpoints by anti-PD-L1 antibodies. and/or (3) increasing XCR1+ DC to SIRPα+ DC ratios by Flt3L administration all led to an increase of functional virus-specific CD8+ T cells with enhanced virus control. Importantly, the functional gain of CD8+ T cells, mainly $T_{PEX}2$, $T_{EX}$INT, and $T_{EX}$TER, was dependent on XCR1+ DCs in all cases. These data not only propose different immunotherapy options to treat chronic virus infections but also highlight the key role of XCR1+ DCs and their differential effects on exhausted CD8+ T cell subsets for therapy success.

XCR1+ and SIRPα+ DCs behave differently with respect to virus susceptibility and immune regulatory functionality during chronic LCMV infection. In the chronic infection phase, XCR1+ DCs expressed the ligands CD40, CD80, and CD86 necessary for regulating exhausted CD8+ T cell functioning through costimulatory pathways[64–66] as well as the cytokines CXCL-9 and IL-12(p40) demonstrating that they are capable to attract T cells and promote their differentiation toward an effector phenotype.[59,67,68] In particular, IL-12 signaling was required for successful anti-PD-L1 treatment in chronic infection (Figures 3E–3I), which is well in line with previous observations in cancer therapy.[60] In contrast, SIRPα+ DCs had lower levels of activation markers but higher levels of PD-L1 and were more susceptible to infection. When being expanded by Flt3L in the absence of XCR1+ DCs, we observed a reduction of $T_{PEX}$ expansion triggered by anti-PD-L1 and an increase in terminal differentiation. Together this suggests that both DC subtypes are part of the homeostatic control mechanism within lymphatic tissue that balances effector function and differentiation of the exhausted CD8+ T cell subsets. It implies that either expansion of XCR1+ DCs or inhibition of SIRPα+ DCs could be of therapeutic use. Evidence for both strategies have been suggested in the context of cancer immunotherapy[69–72] and they seem to apply for chronic infection control as well.

The observation that proliferation and effector function of exhausted antigen-specific CD8+ T cells in chronic LCMV infection are regulated in a segregated manner is consistent with the concept of "feedback-regulated balance of growth and differentiation" by Grossman and Paul.[73] This concept describes the feedbacks that regulate the intensity of proliferation, differentiation and death of antigen-specific T cells and explains the kinetics of expansion upon immunization.[74,75] It was hypothesized that these T cell responses might be driven as well as limited by competition for cytokines or by the action of specialized regulatory elements while clustered around antigen-presenting DCs. Importantly, the specific characterization of the hypothetical cells and molecules involved in the regulation was awaiting definite experimental clarification. Our study here may suggest DC subsets to represent part of those biological control elements that implement the intracluster feedback regulation. Further studies along this concept deserve systematic analyses.

Our findings that XCR1+ DCs are indispensable for anti-PD-L1 immunotherapy during a chronic viral infection are in line with prior studies in the context of cancer therapies.[41,42] Importantly, this requirement for XCR1+ DCs was linked to the functional gain of exhausted CD8+ T cell subpopulations but not their proliferation. This could be explained by the ability of $T_{PEX}$ cells to maintain their proliferative capacities intrinsically through B cell- and monocyte-derived IL-27[76,77] and independent from DC and CD4+ T cell help.[78] In addition, XCR1+ DCs reduced differentiation of the CD8+ T cell subsets toward terminal exhaustion, an observation that was also very recently reported by Dähling and colleagues.[63] Anti-PD-L1 therapy in the absence of XCR1+ DCs only induced CD8+ T cell proliferation without a gain in functionality and without better virus control. This indicated that XCR1+ DC numbers may limit treatment success in certain conditions and that an increase in that DC subset would be beneficial. Indeed, this was observed in cancer treatment when combining Flt3L, radiotherapy, and a TLR3/CD40 agonist by *in situ* administration.[43,79] However, in our experiments with chronic LCMV infection and systemic Flt3L delivery, the functional gain of CD8+ T cells was counterbalanced by a reduction in their absolute numbers and the expansion of SIRPα+ DCs that are a preferred virus infection target.

The differential dependence of the exhausted CD8+ T cell subsets on XCR1+ DCs for their functional activation is not yet completely understood. Activation requires direct contact of T cell receptors with epitope-loaded MHC molecules on antigen-presenting cells. During chronic LCMV infection, XCR1+ DCs are present both in the T cell zone and in the red pulp of the spleen where they can contact both $T_{PEX}$ and $T_{EX}$, respectively.[9,63] Upon anti-PD-L1 treatment, both XCR1+ DCs and virus-specific T cells reorganize around the marginal zone.[63] Therefore, the fact that $T_{PEX}1$ are not activated by XCR1+ DCs during anti-PD-L1 treatment cannot be explained by location alone but may be due to their presence in specialized niches that help maintain their quiescent and stem-like properties, for example within the T cell zone in chronic infection,[13,80] or in dense antigen-presenting cell niches within tumors.[81] Direct evidence for a differential dynamic and localized interplay between XCR1+ DCs and exhausted CD8+ T cell subsets is still lacking and deserves further investigation.

The critical importance of XCR1+ DCs for the functional gain of exhausted CD8+ T cell subsets may direct options for immunotherapeutic intervention strategies against chronic virus infections. Targeting virus antigen to XCR1+DCs, i.e., by linking a viral protein to the DC-attracting chemokine XCL1, or expanding XCR1+DC numbers by Flt3L, augmented exhausted CD8+ T cell functions and led to better virus control. The same was achieved when blocking PD-L1-mediated signaling. Combining

(F and G) Percentage of Ki-67+ $T_{PEX}1$, $T_{PEX}2$, $T_{EX}$INT, and $T_{EX}$ TER (F) and subset frequency within gp33-tet+ exhausted CD8+ T cells (G).
(H–K) Representative plots and frequency of IFNγ-producing and TNFα-producing exhausted CD8+ T cell subsets.
Data shown are the mean ± SEM from 4–6 mice per group. Statistical analysis was performed using one-way ANOVA with Tukey's multiple comparisons (ns = not significant; *p < 0.05; **p < 0.01; ***p < 0.001; ****p < 0.0001).

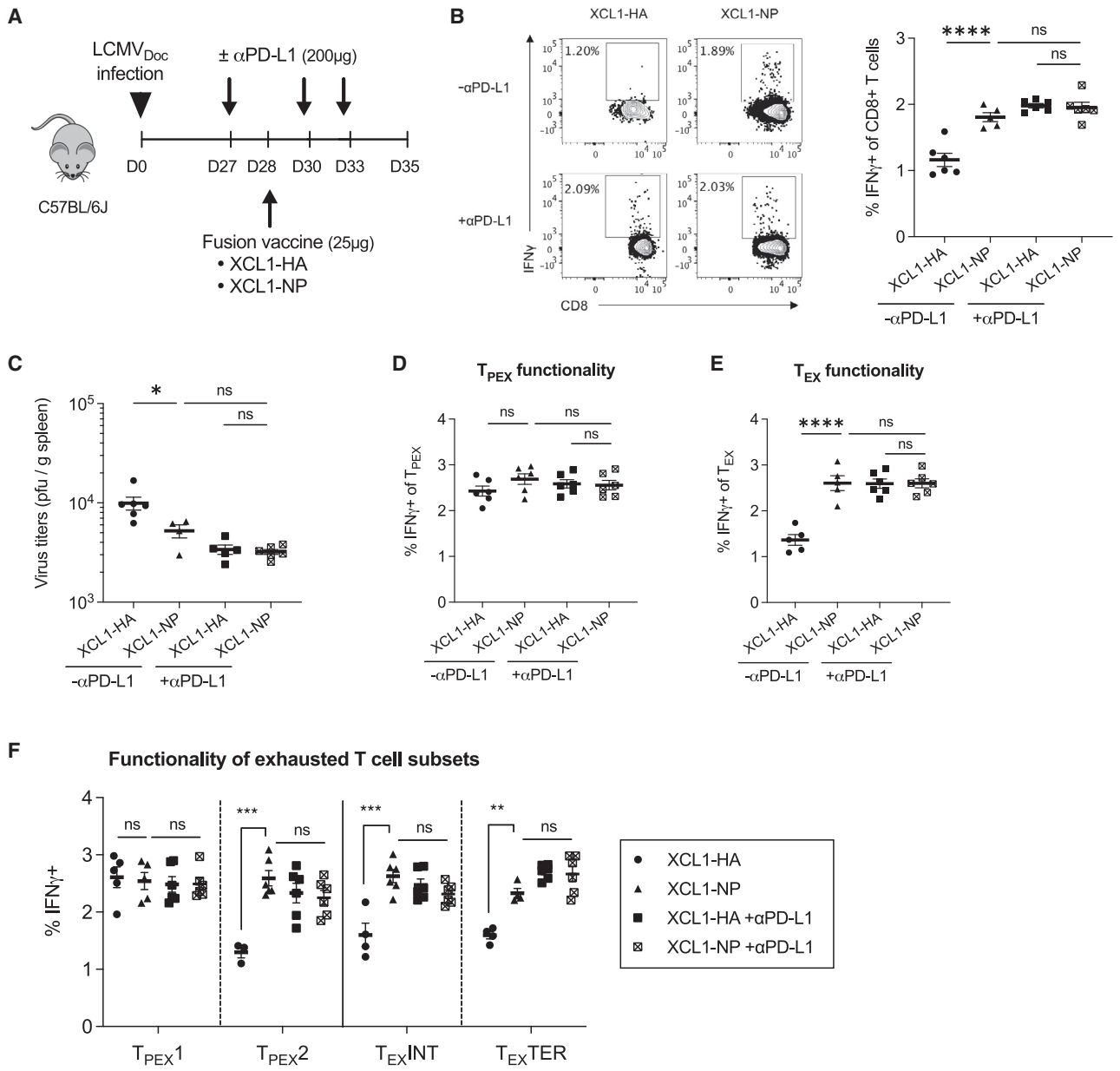


**Figure 5. Combination of XCR1+ DC antigen targeting and anti-PD-L1 treatment in chronic LCMV infection**

(A) Schematic representation of fusion vaccine and DT treatment regimens in C57BL/6J mice. Chronic infected and anti-PD-L1 treated (+αPD-L1) or untreated (−αPD-L1) mice were vaccinated with the corresponding fusion vaccines and killed at day 35 p.i.

(B–F) Spleens were harvested to quantify the percentage of $NP_{396-404}$-specific IFNγ-producing CD8+ T cells (B), viral loads (C), and frequencies of IFNγ-producing exhausted T cell subsets (D–F).

Data shown are the mean ± SEM from six mice per group. Statistical analysis was performed using one-way ANOVA with Tukey's multiple comparisons (ns = not significant; *p < 0.05; **p < 0.01; ***p < 0.001; ****p < 0.0001).

treatments, for example, administration of anti-PD-L1 together with antigen targeting to XCR1+ DCs or with Flt3L injection may further increase T cell functionality. However, the extent of this and its benefit for virus control may depend on the properties of the infecting virus. In the experimental infection system used here, in which LCMV infects lymphatic tissue and uses antigen-presenting cells including SIRPα+ DCs as target cells, the chronic infection state may have sufficient antigen levels in the spleen so that additional targeting to XCR1+ DCs only had a minor effect. Likewise, the T cell functionality improvement by increasing the number of XCR1+ DCs by Flt3L may be compensated by the increase of SIRPα+ DCs that represent new virus target cells and help virus expansion. The respective implications for the immunotherapy of chronic virus infections like those

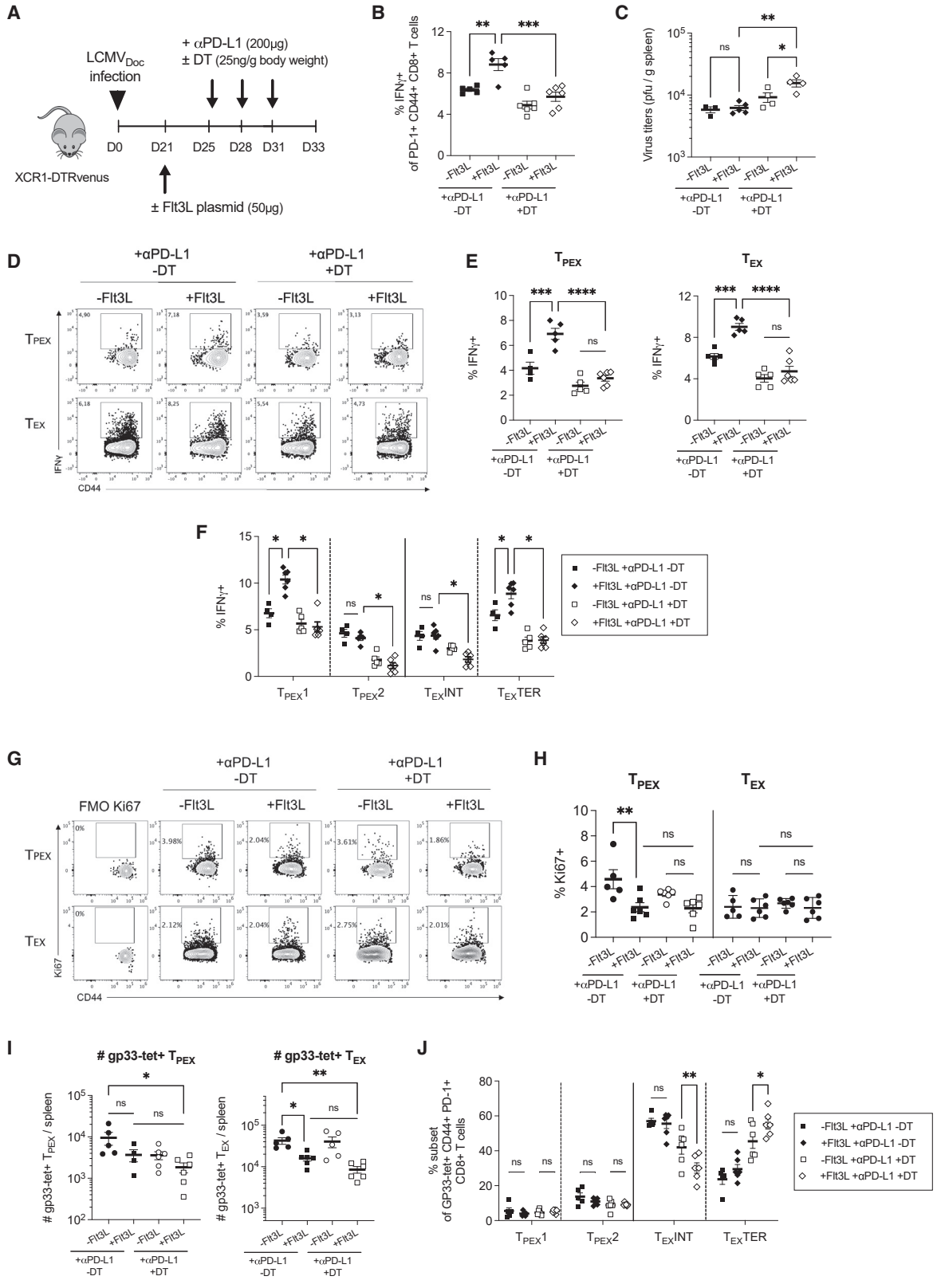


*(legend on next page)*

with HIV or hepatitis B virus (HBV) in humans are unclear but should clearly be addressed.

While the immunotherapy of virus infections is an old concept, it gained a lot of attention in recent years due to the success of checkpoint inhibitors in cancer treatment.[23] However, in most of these trials, HIV or chronic HBV or HCV infections were exclusion criteria due to concerns regarding safety, efficacy, and tolerance of checkpoint inhibitors when combined with antiviral therapy.[82] Nonetheless, trial results with few chronic virus-infected patients did not support such concerns and suggest a benefit at least for some of the patients.[28,83,84] With the data provided here in the chronic LCMV infection model in mice, especially the combination of anti-PD-L1 with virus antigen targeting to cross-presenting DC would be an interesting therapy option for HIV-infected individuals. With the virus load controlled by antiretroviral therapy, the likelihood of exhausted regulatory T cell expansion would be reduced[85] and cross-presenting DC-targeting vaccines might then redirect HIV-specific cytotoxic CD8+ T cell (CTL) responses to conserved epitopes within the patient.[86] Given that all the elements of such a therapy strategy are in place, including human cross-presenting DC-targeting constructs,[87] conserved HIV CTL epitope immunogens[86] and a variety of available checkpoint inhibitors, it seems a feasible and well supported immunotherapy approach.

### Limitations of the study

The dynamic interplay between the DC populations and the exhausted CD8+ T cell subsets that finally determine differential T cell activation is not resolved. Tools are still lacking that allow capturing and/or blocking exhausted T cell differentiation *in vivo*. Furthermore, specific depletion of SIRP$\alpha$+ DCs is not yet possible. Our attempts to co-localize the DC subsets with $T_{PEX}$ cells after adoptive transfer of $T_{PEX}$ into chronic LCMV-infected mice resulted in too low cell numbers to reach a conclusion.

## STAR★METHODS

Detailed methods are provided in the online version of this paper and include the following:

- KEY RESOURCES TABLE
- RESOURCE AVAILABILITY
  - Lead contact
  - Materials availability
  - Data and code availability
- EXPERIMENTAL MODEL AND SUBJECT DETAILS
  - Mice
  - Viruses and infections
- METHOD DETAILS
  - Cell preparation, flow cytometry and cell sorting
  - Intracellular cytokine staining
  - Virus load quantification
  - *In vivo* anti-PD-L1 antibody treatment
  - *In vivo* cell depletion
  - *In vivo* transfection of human Flt3L
  - *In vivo* neutralization of CXCL-9 and IL-12
  - Electroporation of Xcl1-targeted fusion vaccines
- QUANTIFICATION AND STATISTICAL ANALYSIS

### SUPPLEMENTAL INFORMATION

Supplemental information can be found online at https://doi.org/10.1016/j.celrep.2023.112123.

### ACKNOWLEDGMENTS

We thank the Flow Cytometry Unit (Universitat Pompeu Fabra) for excellent technical support. This work was supported by grants from the Spanish Ministry of Science and Innovation (grant No. PID2019-106323RB-I00 AEI// 10.13039/501100011033), the "Unidad de Excelencia María de Maeztu" funded by the MCIN and the AEI (DOI: 10.13039/501100011033; Ref: CEX2018-000792-M), "la Caixa" Foundation (HR17-00199), the Russian Science Foundation (grant No. 18-11-00171), and the Research Council of Norway (grant No. 250884).

### AUTHOR CONTRIBUTIONS

Conceptualization, J.A., G.B., and A.M.; Investigation, E.D.-V., V.C., R.I., M.P., and P.C.R.; Resources, E.F., Q.C., T.K., and K.T.; Writing, E.D.-V., J.A., and A.M.; Visualization, E.D.-V.; Project Administration, J.A.; Funding acquisition, J.A., G.B., and A.M.

### DECLARATION OF INTERESTS

The authors declare no competing interests.

### INCLUSION AND DIVERSITY

We support inclusive, diverse, and equitable conduct of research.

Received: April 29, 2021
Revised: December 11, 2022
Accepted: January 30, 2023

### REFERENCES

1. McLane, L.M., Abdel-Hakeem, M.S., and Wherry, E.J. (2019). CD8 T cell exhaustion during chronic viral infection and cancer. Annu. Rev. Immunol. *37*, 457–495. https://doi.org/10.1146/annurev-immunol-041015-055318.
2. Alfei, F., Kanev, K., Hofmann, M., Wu, M., Ghoneim, H.E., Roelli, P., Utzschneider, D.T., von Hoesslin, M., Cullen, J.G., Fan, Y., et al. (2019). TOX reinforces the phenotype and longevity of exhausted T cells in chronic

**Figure 6. Combination of anti-PD-L1 treatment with Flt3L-mediated expansion of XCR1+ DCs**

(A) Schematic representation of Flt3L and DT treatment regimens in XCR1-DTRvenus mice during anti-PD-L1 immunotherapy. Chronic infected and anti-PD-L1 treated mice were transfected with Flt3L-expressing plasmid in the presence (−DT) or absence (+DT) of XCR1+ DCs, and killed at day 33 p.i.

(B and C) Spleens were harvested to quantify the percentage of $GP_{33-41}$-specific IFN$\gamma$-producing PD-1+ CD44+ CD8+ T cells (B) and viral loads (C).

(D–H) Representative plots and frequencies of $GP_{33-41}$-specific IFN$\gamma$-producing (D–F) and proliferating (G and H) exhausted CD8+ T cell subsets.

(I) Absolute numbers of gp33-tet+ $T_{PEX}$ and $T_{EX}$ in spleen.

(J) Percentages of $T_{PEX}1$, $T_{PEX}2$, $T_{EX}$INT, and $T_{EX}$TER within gp33-tet+ exhausted CD8+ T cells.

Data shown are the mean ± SEM from 5–7 mice per group. Statistical analysis was performed using one-way ANOVA with Tukey's multiple comparisons (ns = not significant; *p > 0.05; **p < 0.01; ***p < 0.001; ****p < 0.0001).

viral infection. Nature *571*, 265–269. https://doi.org/10.1038/s41586-019-1326-9.

3. Khan, O., Giles, J.R., McDonald, S., Manne, S., Ngiow, S.F., Patel, K.P., Werner, M.T., Huang, A.C., Alexander, K.A., Wu, J.E., et al. (2019). TOX transcriptionally and epigenetically programs CD8 T cell exhaustion. Nature *571*, 211–218. https://doi.org/10.1038/s41586-019-1325-x.
4. Seo, H., Chen, J., González-Avalos, E., Samaniego-Castruita, D., Das, A., Wang, Y.H., López-Moyado, I.F., Georges, R.O., Zhang, W., Onodera, A., et al. (2019). TOX and TOX2 transcription factors cooperate with NR4A transcription factors to impose CD8+ T cell exhaustion. Proc. Natl. Acad. Sci. USA *116*, 12410–12415. https://doi.org/10.1073/pnas.1905675116.
5. Utzschneider, D.T., Gabriel, S.S., Chisanga, D., Gloury, R., Gubser, P.M., Vasanthakumar, A., Shi, W., and Kallies, A. (2020). Early precursor T cells establish and propagate T cell exhaustion in chronic infection. Nat. Immunol. *21*, 1256–1266. https://doi.org/10.1038/s41590-020-0760-z.
6. Utzschneider, D.T., Alfei, F., Roelli, P., Barras, D., Chennupati, V., Darbre, S., Delorenzi, M., Pinschewer, D.D., and Zehn, D. (2016). High antigen levels induce an exhausted phenotype in a chronic infection without impairing T cell expansion and survival. J. Exp. Med. *213*, 1819–1834. https://doi.org/10.1084/jem.20150598.
7. Bengsch, B., Ohtani, T., Khan, O., Setty, M., Manne, S., O'Brien, S., Gherardini, P.F., Herati, R.S., Huang, A.C., Chang, K.-M., et al. (2018). Epigenomic-guided mass cytometry profiling reveals disease-specific features of exhausted CD8 T cells. Immunity *48*, 1029–1045.e5. https://doi.org/10.1016/j.immuni.2018.04.026.
8. Im, S.J., Hashimoto, M., Gerner, M.Y., Lee, J., Kissick, H.T., Burger, M.C., Shan, Q., Hale, J.S., Lee, J., Nasti, T.H., et al. (2016). Defining CD8+ T cells that provide the proliferative burst after PD-1 therapy. Nature *537*, 417–421. https://doi.org/10.1038/nature19330.
9. Beltra, J.-C., Manne, S., Abdel-Hakeem, M.S., Kurachi, M., Giles, J.R., Chen, Z., Casella, V., Ngiow, S.F., Khan, O., Huang, Y.J., et al. (2020). Developmental relationships of four exhausted CD8 T cell subsets reveals underlying transcriptional and epigenetic landscape control mechanisms. Immunity *52*, 825–841.e8. https://doi.org/10.1016/j.immuni.2020.04.014.
10. Sandu, I., Cerletti, D., Oetiker, N., Borsa, M., Wagen, F., Spadafora, I., Welten, S.P.M., Stolz, U., Oxenius, A., and Claassen, M. (2020). Landscape of exhausted virus-specific CD8 T cells in chronic LCMV infection. Cell Rep. *32*, 108078. https://doi.org/10.1016/j.celrep.2020.108078.
11. Mylvaganam, G.H., Rios, D., Abdelaal, H.M., Iyer, S., Tharp, G., Mavigner, M., Hicks, S., Chahroudi, A., Ahmed, R., Bosinger, S.E., et al. (2017). Dynamics of SIV-specific CXCR5+ CD8 T cells during chronic SIV infection. Proc. Natl. Acad. Sci. USA *114*, 1976–1981. https://doi.org/10.1073/pnas.1621418114.
12. He, R., Hou, S., Liu, C., Zhang, A., Bai, Q., Han, M., Yang, Y., Wei, G., Shen, T., Yang, X., et al. (2016). Follicular CXCR5- expressing CD8(+) T cells curtail chronic viral infection. Nature *537*, 412–428. https://doi.org/10.1038/nature19317.
13. Leong, Y.A., Chen, Y., Ong, H.S., Wu, D., Man, K., Deleage, C., Minnich, M., Meckiff, B.J., Wei, Y., Hou, Z., et al. (2016). CXCR5(+) follicular cytotoxic T cells control viral infection in B cell follicles. Nat. Immunol. *17*, 1187–1196. https://doi.org/10.1038/ni.3543.
14. Petrovas, C., Ferrando-Martinez, S., Gerner, M.Y., Casazza, J.P., Pegu, A., Deleage, C., Cooper, A., Hataye, J., Andrews, S., Ambrozak, D., et al. (2017). Follicular CD8 T cells accumulate in HIV infection and can kill infected cells in vitro via bispecific antibodies. Sci. Transl. Med. *9*, eaag2285. https://doi.org/10.1126/scitranslmed.aag2285.
15. Li, Y., Tang, L., Guo, L., Chen, C., Gu, S., Zhou, Y., Ye, G., Li, X., Wang, W., Liao, X., et al. (2020). CXCL13-mediated recruitment of intrahepatic CXCR5CD8 T cells favors viral control in chronic HBV infection. J. Hepatol. *72*, 420–430. https://doi.org/10.1016/j.jhep.2019.09.031.
16. Wieland, D., Kemming, J., Schuch, A., Emmerich, F., Knolle, P., Neumann-Haefelin, C., Held, W., Zehn, D., Hofmann, M., and Thimme, R. (2017). TCF1 hepatitis C virus-specific CD8 T cells are maintained after cessation of chronic antigen stimulation. Nat. Commun. *8*, 15050. https://doi.org/10.1038/ncomms15050.
17. Brummelman, J., Mazza, E.M.C., Alvisi, G., Colombo, F.S., Grilli, A., Mikulak, J., Mavilio, D., Alloisio, M., Ferrari, F., Lopci, E., et al. (2018). High-dimensional single cell analysis identifies stem-like cytotoxic CD8 T cells infiltrating human tumors. J. Exp. Med. *215*, 2520–2535. https://doi.org/10.1084/jem.20180684.
18. Miller, B.C., Sen, D.R., Al Abosy, R., Bi, K., Virkud, Y.V., LaFleur, M.W., Yates, K.B., Lako, A., Felt, K., Naik, G.S., et al. (2019). Subsets of exhausted CD8 T cells differentially mediate tumor control and respond to checkpoint blockade. Nat. Immunol. *20*, 326–336. https://doi.org/10.1038/s41590-019-0312-6.
19. Siddiqui, I., Schaeuble, K., Chennupati, V., Fuertes Marraco, S.A., Calderon-Copete, S., Pais Ferreira, D., Carmona, S.J., Scarpellino, L., Gfeller, D., Pradervand, S., et al. (2019). Intratumoral Tcf1+ PD-1+ CD8 T cells with stem-like properties promote tumor control in response to vaccination and checkpoint blockade immunotherapy. Immunity *50*, 195–211.e10. https://doi.org/10.1016/j.immuni.2018.12.021.
20. Barber, D.L., Wherry, E.J., Masopust, D., Zhu, B., Allison, J.P., Sharpe, A.H., Freeman, G.J., and Ahmed, R. (2006). Restoring function in exhausted CD8 T cells during chronic viral infection. Nature *439*, 682–687. https://doi.org/10.1038/nature04444.
21. Pauken, K.E., and Wherry, E.J. (2015). Overcoming T cell exhaustion in infection and cancer. Trends Immunol. *36*, 265–276. https://doi.org/10.1016/j.it.2015.02.008.
22. Zou, W., Wolchok, J.D., and Chen, L. (2016). PD-L1 (B7-H1) and PD-1 pathway blockade for cancer therapy: mechanisms, response biomarkers, and combinations. Sci. Transl. Med. *8*, 328rv4. https://doi.org/10.1126/scitranslmed.aad7118.
23. Ribas, A., and Wolchok, J.D. (2018). Cancer immunotherapy using checkpoint blockade. Science *359*, 1350–1355. https://doi.org/10.1126/science.aar4060.
24. Wykes, M.N., and Lewin, S.R. (2018). Immune checkpoint blockade in infectious diseases. Nat. Rev. Immunol. *18*, 91–104. https://doi.org/10.1038/nri.2017.112.
25. Rajdev, L., Chiao, E.Y., Lensing, S., Little, R.F., Dittmer, D., Einstein, M.H., Haigentz, M., Sparano, J.A., and Mitsuyasu, R.T. (2018). AMC 095 (AIDS malignancy Consortium): A phase I study of ipilimumab (IPI) and nivolumab (NIVO) in advanced HIV associated solid tumors (ST) with expansion cohorts in HIV associated solid tumors and classical Hodgkin lymphoma (cHL). J. Clin. Oncol. *36*, TPS2597. https://doi.org/10.1200/JCO.2018.36.15_suppl.TPS2597.
26. Uldrick, T.S., Gonçalves, P.H., Abdul-Hay, M., Claeys, A.J., Emu, B., Ernstoff, M.S., Fling, S.P., Fong, L., Kaiser, J.C., Lacroix, A.M., et al. (2019). assessment of the safety of pembrolizumab in patients with HIV and advanced cancer-A phase 1 study. JAMA Oncol. *5*, 1332–1339. https://doi.org/10.1001/jamaoncol.2019.2244.
27. Blanch-Lombarte, O., Gálvez, C., Revollo, B., Jiménez-Moyano, E., Llibre, J.M., Manzano, J.L., Boada, A., Dalmau, J., E Speiser, D., Clotet, B., et al. (2019). Enhancement of antiviral CD8 T-cell responses and complete remission of metastatic melanoma in an HIV-1-Infected subject treated with pembrolizumab. J. Clin. Med. *8*, 2089. https://doi.org/10.3390/jcm8122089.
28. Gonzalez-Cao, M., Morán, T., Dalmau, J., Garcia-Corbacho, J., Bracht, J.W.P., Bernabe, R., Juan, O., de Castro, J., Blanco, R., Drozdowskyj, A., et al. (2020). Assessment of the feasibility and safety of durvalumab for treatment of solid tumors in patients with HIV-1 infection: the phase 2 DURVAST study. JAMA Oncol. *6*, 1063–1067. https://doi.org/10.1001/jamaoncol.2020.0465.
29. Kallies, A., Zehn, D., and Utzschneider, D.T. (2020). Precursor exhausted T cells: key to successful immunotherapy? Nat. Rev. Immunol. *20*, 128–136. https://doi.org/10.1038/s41577-019-0223-7.
30. Verma, V., Shrimali, R.K., Ahmad, S., Dai, W., Wang, H., Lu, S., Nandre, R., Gaur, P., Lopez, J., Sade-Feldman, M., et al. (2019). PD-1 blockade in

subprimed CD8 cells induces dysfunctional PD-1+ CD38+ cells and anti-PD-1 resistance. Nat. Immunol. *20*, 1231–1243. https://doi.org/10.1038/s41590-019-0441-y.

31. Eickhoff, S., Brewitz, A., Gerner, M.Y., Klauschen, F., Komander, K., Hemmi, H., Garbi, N., Kaisho, T., Germain, R.N., and Kastenmüller, W. (2015). Robust anti-viral immunity requires multiple distinct T cell-dendritic cell interactions. Cell *162*, 1322–1337. https://doi.org/10.1016/j.cell.2015.08.004.

32. Brewitz, A., Eickhoff, S., Dähling, S., Quast, T., Bedoui, S., Kroczek, R.A., Kurts, C., Garbi, N., Barchet, W., Iannacone, M., et al. (2017). CD8 T cells orchestrate pDC-XCR1 dendritic cell spatial and functional cooperativity to optimize priming. Immunity *46*, 205–219. https://doi.org/10.1016/j.immuni.2017.01.003.

33. Ferris, S.T., Durai, V., Wu, R., Theisen, D.J., Ward, J.P., Bern, M.D., Davidson, J.T., Bagadia, P., Liu, T., Briseño, C.G., et al. (2020). cDC1 prime and are licensed by CD4 T cells to induce anti-tumour immunity. Nature *584*, 624–629. https://doi.org/10.1038/s41586-020-2611-3.

34. Dorner, B.G., Dorner, M.B., Zhou, X., Opitz, C., Mora, A., Güttler, S., Hutloff, A., Mages, H.W., Ranke, K., Schaefer, M., et al. (2009). Selective expression of the chemokine receptor XCR1 on cross-presenting dendritic cells determines cooperation with CD8+ T cells. Immunity *31*, 823–833. https://doi.org/10.1016/j.immuni.2009.08.027.

35. Crozat, K., Guiton, R., Contreras, V., Feuillet, V., Dutertre, C.-A., Ventre, E., Vu Manh, T.-P., Baranek, T., Storset, A.K., Marvel, J., et al. (2010). The XC chemokine receptor 1 is a conserved selective marker of mammalian cells homologous to mouse CD8alpha+ dendritic cells. J. Exp. Med. *207*, 1283–1292. https://doi.org/10.1084/jem.20100223.

36. Böttcher, J.P., Bonavita, E., Chakravarty, P., Blees, H., Cabeza-Cabrerizo, M., Sammicheli, S., Rogers, N.C., Sahai, E., Zelenay, S., and Reis E Sousa, C. (2018). NK cells stimulate recruitment of cDC1 into the tumor microenvironment promoting cancer immune control. Cell *172*, 1022–1037.e14. https://doi.org/10.1016/j.cell.2018.01.004.

37. Argilaguet, J., Pedragosa, M., Esteve-Codina, A., Riera, G., Vidal, E., Peligero-Cruz, C., Casella, V., Andreu, D., Kaisho, T., Bocharov, G., et al. (2019). Systems analysis reveals complex biological processes during virus infection fate decisions. Genome Res. *29*, 907–919. https://doi.org/10.1101/gr.241372.118.

38. Alcántara-Hernández, M., Leylek, R., Wagar, L.E., Engleman, E.G., Keler, T., Marinkovich, M.P., Davis, M.M., Nolan, G.P., and Idoyaga, J. (2017). High-Dimensional phenotypic mapping of human dendritic cells reveals interindividual variation and tissue specialization. Immunity *47*, 1037–1050.e6. https://doi.org/10.1016/j.immuni.2017.11.001.

39. Dutertre, C.-A., Jourdain, J.-P., Rancez, M., Amraoui, S., Fossum, E., Bogen, B., Sanchez, C., Couëdel-Courteille, A., Richard, Y., Dalod, M., et al. (2014). TLR3-responsive, XCR1+, CD141(BDCA-3)+/CD8α+-equivalent dendritic cells uncovered in healthy and simian immunodeficiency virus-infected rhesus macaques. J. Immunol. *192*, 4697–4708. https://doi.org/10.4049/jimmunol.1302448.

40. Roberts, E.W., Broz, M.L., Binnewies, M., Headley, M.B., Nelson, A.E., Wolf, D.M., Kaisho, T., Bogunovic, D., Bhardwaj, N., and Krummel, M.F. (2016). Critical role for CD103/CD141 dendritic cells bearing CCR7 for tumor antigen trafficking and priming of T cell immunity in melanoma. Cancer Cell *30*, 324–336. https://doi.org/10.1016/j.ccell.2016.06.003.

41. Spranger, S., Dai, D., Horton, B., and Gajewski, T.F. (2017). Tumor-Residing Batf3 dendritic cells are required for effector T cell trafficking and adoptive T cell therapy. Cancer Cell *31*, 711–723.e4. https://doi.org/10.1016/j.ccell.2017.04.003.

42. Salmon, H., Idoyaga, J., Rahman, A., Leboeuf, M., Remark, R., Jordan, S., Casanova-Acebes, M., Khudoynazarova, M., Agudo, J., Tung, N., et al. (2016). Expansion and activation of CD103(+) dendritic cell progenitors at the tumor site enhances tumor responses to therapeutic PD-L1 and BRAF inhibition. Immunity *44*, 924–938. https://doi.org/10.1016/j.immuni.2016.03.012.

43. Hammerich, L., Marron, T.U., Upadhyay, R., Svensson-Arvelund, J., Dhainaut, M., Hussein, S., Zhan, Y., Ostrowski, D., Yellin, M., Marsh, H., et al. (2019). Systemic clinical tumor regressions and potentiation of PD1 blockade with in situ vaccination. Nat. Med. *25*, 814–824. https://doi.org/10.1038/s41591-019-0410-x.

44. Saito, Y., Respatika, D., Komori, S., Washio, K., Nishimura, T., Kotani, T., Murata, Y., Okazawa, H., Ohnishi, H., Kaneko, Y., et al. (2017). SIRPα+ dendritic cells regulate homeostasis of fibroblastic reticular cells via TNF receptor ligands in the adult spleen. Proc. Natl. Acad. Sci. USA *114*, E10151–E10160. https://doi.org/10.1073/pnas.1711345114.

45. Calabro, S., Liu, D., Gallman, A., Nascimento, M.S.L., Yu, Z., Zhang, T.-T., Chen, P., Zhang, B., Xu, L., Gowthaman, U., et al. (2016). Differential intrasplenic migration of dendritic cell subsets tailors adaptive immunity. Cell Rep. *16*, 2472–2485. https://doi.org/10.1016/j.celrep.2016.07.076.

46. Liu, Q., Wen, W., Tang, L., Qin, C.J., Lin, Y., Zhang, H.L., Wu, H., Ashton, C., Wu, H.P., Ding, J., et al. (2016). Inhibition of SIRPα in dendritic cells potentiates potent antitumor immunity. OncoImmunology *5*, e1183850. https://doi.org/10.1080/2162402X.2016.1183850.

47. Gauttier, V., Pengam, S., Durand, J., Biteau, K., Mary, C., Morello, A., Néel, M., Porto, G., Teppaz, G., Thepenier, V., et al. (2020). Selective SIRPα blockade reverses tumor T cell exclusion and overcomes cancer immunotherapy resistance. J. Clin. Invest. *130*, 6109–6123. https://doi.org/10.1172/JCI135528.

48. Richter, K., Perriard, G., and Oxenius, A. (2013). Reversal of chronic to resolved infection by IL-10 blockade is LCMV strain dependent. Eur. J. Immunol. *43*, 649–654. https://doi.org/10.1002/eji.201242887.

49. Ng, C.T., and Oldstone, M.B.A. (2012). Infected CD8α- dendritic cells are the predominant source of IL-10 during establishment of persistent viral infection. Proc. Natl. Acad. Sci. USA *109*, 14116–14121. https://doi.org/10.1073/pnas.1211910109.

50. Sevilla, N., McGavern, D.B., Teng, C., Kunz, S., and Oldstone, M.B.A. (2004). Viral targeting of hematopoietic progenitors and inhibition of DC maturation as a dual strategy for immune subversion. J. Clin. Invest. *113*, 737–745. https://doi.org/10.1172/JCI20243.

51. Macal, M., Lewis, G.M., Kunz, S., Flavell, R., Harker, J.A., and Zúñiga, E.I. (2012). Plasmacytoid dendritic cells are productively infected and activated through TLR-7 early after arenavirus infection. Cell Host Microbe *11*, 617–630. https://doi.org/10.1016/j.chom.2012.04.017.

52. Ng, C.T., Sullivan, B.M., Teijaro, J.R., Lee, A.M., Welch, M., Rice, S., Sheehan, K.C.F., Schreiber, R.D., and Oldstone, M.B.A. (2015). Blockade of interferon Beta, but not interferon alpha, signaling controls persistent viral infection. Cell Host Microbe *17*, 653–661. https://doi.org/10.1016/j.chom.2015.04.005.

53. Silvin, A., Yu, C.I., Lahaye, X., Imperatore, F., Brault, J.-B., Cardinaud, S., Becker, C., Kwan, W.-H., Conrad, C., Maurin, M., et al. (2017). Constitutive resistance to viral infection in human CD141 dendritic cells. Sci. Immunol. *2*, eaai8071. https://doi.org/10.1126/sciimmunol.aai8071.

54. Iwabuchi, R., Ikeno, S., Kobayashi-Ishihara, M., Takeyama, H., Ato, M., Tsunetsugu-Yokota, Y., and Terahara, K. (2018). Introduction of human flt3-L and GM-CSF into humanized mice enhances the reconstitution and maturation of myeloid dendritic cells and the development of Foxp3 + CD4 + T cells. Front. Immunol. *9*, 1042. https://doi.org/10.3389/fimmu.2018.01042.

55. Wherry, E.J., Blattman, J.N., Murali-Krishna, K., van der Most, R., and Ahmed, R. (2003). Viral persistence alters CD8 T-cell immunodominance and tissue distribution and results in distinct stages of functional impairment. J. Virol. *77*, 4911–4927. https://doi.org/10.1128/jvi.77.8.4911-4927.2003.

56. Yamazaki, C., Sugiyama, M., Ohta, T., Hemmi, H., Hamada, E., Sasaki, I., Fukuda, Y., Yano, T., Nobuoka, M., Hirashima, T., et al. (2013). Critical roles of a dendritic cell subset expressing a chemokine receptor, XCR1. J. Immunol. *190*, 6071–6082. https://doi.org/10.4049/jimmunol.1202798.

57. Ha, S.J., Mueller, S.N., Wherry, E.J., Barber, D.L., Aubert, R.D., Sharpe, A.H., Freeman, G.J., and Ahmed, R. (2008). Enhancing therapeutic

vaccination by blocking PD-1-mediated inhibitory signals during chronic infection. J. Exp. Med. *205*, 543–555. https://doi.org/10.1084/jem.20071949.

58. Fossum, E., Grødeland, G., Terhorst, D., Tveita, A.A., Vikse, E., Mjaaland, S., Henri, S., Malissen, B., and Bogen, B. (2015). Vaccine molecules targeting Xcr1 on cross-presenting DCs induce protective CD8+ T-cell responses against influenza virus. Eur. J. Immunol. *45*, 624–635. https://doi.org/10.1002/eji.201445080.

59. Danilo, M., Chennupati, V., Silva, J.G., Siegert, S., and Held, W. (2018). Suppression of tcf1 by inflammatory cytokines facilitates effector CD8 T cell differentiation. Cell Rep. *22*, 2107–2117. https://doi.org/10.1016/j.celrep.2018.01.072.

60. Garris, C.S., Arlauckas, S.P., Kohler, R.H., Trefny, M.P., Garren, S., Piot, C., Engblom, C., Pfirschke, C., Siwicki, M., Gungabeesoon, J., et al. (2018). Successful anti-PD-1 cancer immunotherapy requires T cell-dendritic cell crosstalk involving the cytokines IFN-γ and IL-12. Immunity *49*, 1148–1161.e7. https://doi.org/10.1016/j.immuni.2018.09.024.

61. Kurachi, M., Kurachi, J., Suenaga, F., Tsukui, T., Abe, J., Ueha, S., Tomura, M., Sugihara, K., Takamura, S., Kakimi, K., and Matsushima, K. (2011). Chemokine receptor CXCR3 facilitates CD8(+) T cell differentiation into short-lived effector cells leading to memory degeneration. J. Exp. Med. *208*, 1605–1620. https://doi.org/10.1084/jem.20102101.

62. Ozga, A.J., Chow, M.T., Lopes, M.E., Servis, R.L., Di Pilato, M., Dehio, P., Lian, J., Mempel, T.R., and Luster, A.D. (2022). CXCL10 chemokine regulates heterogeneity of the CD8+ T cell response and viral set point during chronic infection. Immunity *55*, 82–97.e8. https://doi.org/10.1016/j.immuni.2021.11.002.

63. Dähling, S., Mansilla, A.M., Knöpper, K., Grafen, A., Utzschneider, D.T., Ugur, M., Whitney, P.G., Bachem, A., Arampatzi, P., Imdahl, F., et al. (2022). Type 1 conventional dendritic cells maintain and guide the differentiation of precursors of exhausted T cells in distinct cellular niches. Immunity *55*, 656–670.e8. https://doi.org/10.1016/j.immuni.2022.03.006.

64. Isogawa, M., Chung, J., Murata, Y., Kakimi, K., and Chisari, F.V. (2013). CD40 activation rescues antiviral $CD8^+$ T cells from PD-1-mediated exhaustion. PLoS Pathog. *9*, e1003490. https://doi.org/10.1371/journal.ppat.1003490.

65. Kamphorst, A.O., Wieland, A., Nasti, T., Yang, S., Zhang, R., Barber, D.L., Konieczny, B.T., Daugherty, C.Z., Koenig, L., Yu, K., et al. (2017). Rescue of exhausted CD8 T cells by PD-1-targeted therapies is CD28-dependent. Science *355*, 1423–1427. https://doi.org/10.1126/science.aaf0683.

66. Hui, E., Cheung, J., Zhu, J., Su, X., Taylor, M.J., Wallweber, H.A., Sasmal, D.K., Huang, J., Kim, J.M., Mellman, I., and Vale, R.D. (2017). T cell costimulatory receptor CD28 is a primary target for PD-1-mediated inhibition. Science *355*, 1428–1433. https://doi.org/10.1126/science.aaf1292.

67. Sung, J.H., Zhang, H., Moseman, E.A., Alvarez, D., Iannacone, M., Henrickson, S.E., de la Torre, J.C., Groom, J.R., Luster, A.D., and von Andrian, U.H. (2012). Chemokine guidance of central memory T cells is critical for antiviral recall responses in lymph nodes. Cell *150*, 1249–1263. https://doi.org/10.1016/j.cell.2012.08.015.

68. Keppler, S.J., Theil, K., Vucikuja, S., and Aichele, P. (2009). Effector T-cell differentiation during viral and bacterial infections: role of direct IL-12 signals for cell fate decision of CD8(+) T cells. Eur. J. Immunol. *39*, 1774–1783. https://doi.org/10.1002/eji.200839093.

69. Sanchez-Paulete, A.R., Labiano, S., Rodriguez-Ruiz, M.E., Azpilikueta, A., Etxeberria, I., Bolaños, E., Lang, V., Rodriguez, M., Aznar, M.A., Jure-Kunkel, M., and Melero, I. (2016). Deciphering CD137 (4-1BB) signaling in T-cell costimulation for translation into successful cancer immunotherapy. Eur. J. Immunol. *46*, 513–522. https://doi.org/10.1002/eji.201445388.

70. Lai, J., Mardiana, S., House, I.G., Sek, K., Henderson, M.A., Giuffrida, L., Chen, A.X.Y., Todd, K.L., Petley, E.V., Chan, J.D., et al. (2020). Adoptive cellular therapy with T cells expressing the dendritic cell growth factor Flt3L drives epitope spreading and antitumor immunity. Nat. Immunol. *21*, 914–926. https://doi.org/10.1038/s41590-020-0676-7.

71. Willingham, S.B., Volkmer, J.-P., Gentles, A.J., Sahoo, D., Dalerba, P., Mitra, S.S., Wang, J., Contreras-Trujillo, H., Martin, R., Cohen, J.D., et al. (2012). The CD47-signal regulatory protein alpha (SIRPα) interaction is a therapeutic target for human solid tumors. Proc. Natl. Acad. Sci. USA *109*, 6662–6667. https://doi.org/10.1073/pnas.1121623109.

72. Veillette, A., and Chen, J. (2018). SIRPα-CD47 immune checkpoint blockade in anticancer therapy. Trends Immunol. *39*, 173–184. https://doi.org/10.1016/j.it.2017.12.005.

73. Grossman, Z., Min, B., Meier-Schellersheim, M., and Paul, W.E. (2004). Concomitant regulation of T-cell activation and homeostasis. Nat. Rev. Immunol. *4*, 387–395. https://doi.org/10.1038/nri1355.

74. Quiel, J., Caucheteux, S., Laurence, A., Singh, N.J., Bocharov, G., Ben-Sasson, S.Z., Grossman, Z., and Paul, W.E. (2011). Antigen-stimulated CD4 T-cell expansion is inversely and log-linearly related to precursor number. Proc. Natl. Acad. Sci. USA *108*, 3312–3317. https://doi.org/10.1073/pnas.1018525108.

75. Bocharov, G., Quiel, J., Luzyanina, T., Alon, H., Chiglintsev, E., Chereshnev, V., Meier-Schellersheim, M., Paul, W.E., and Grossman, Z. (2011). Feedback regulation of proliferation vs. differentiation rates explains the dependence of CD4 T-cell expansion on precursor number. Proc. Natl. Acad. Sci. USA *108*, 3318–3323. https://doi.org/10.1073/pnas.1019706108.

76. Huang, Z., Zak, J., Pratumchai, I., Shaabani, N., Vartabedian, V.F., Nguyen, N., Wu, T., Xiao, C., and Teijaro, J.R. (2019). IL-27 promotes the expansion of self-renewing CD8+ T cells in persistent viral infection. J. Exp. Med. *216*, 1791–1808. https://doi.org/10.1084/jem.20190173.

77. Pratumchai, I., Zak, J., Huang, Z., Min, B., Oldstone, M.B.A., and Teijaro, J.R. (2022). B cell-derived IL-27 promotes control of persistent LCMV infection. Proc. Natl. Acad. Sci. USA *119*, e2116741119. https://doi.org/10.1073/pnas.2116741119.

78. Kanev, K., Wu, M., Drews, A., Roelli, P., Wurmser, C., von Hösslin, M., and Zehn, D. (2019). Proliferation-competent Tcf1+ CD8 T cells in dysfunctional populations are CD4 T cell help independent. Proc. Natl. Acad. Sci. USA *116*, 20070–20076. https://doi.org/10.1073/pnas.1902701116.

79. Oba, T., Long, M.D., Keler, T., Marsh, H.C., Minderman, H., Abrams, S.I., Liu, S., and Ito, F. (2020). Overcoming primary and acquired resistance to anti-PD-L1 therapy by induction and activation of tumor-residing cDC1s. Nat. Commun. *11*, 5415. https://doi.org/10.1038/s41467-020-19192-z.

80. Im, S.J., Konieczny, B.T., Hudson, W.H., Masopust, D., and Ahmed, R. (2020). PD-1+ stemlike CD8 T cells are resident in lymphoid tissues during persistent LCMV infection. Proc. Natl. Acad. Sci. USA *117*, 4292–4299. https://doi.org/10.1073/pnas.1917298117.

81. Jansen, C.S., Prokhnevska, N., Master, V.A., Sanda, M.G., Carlisle, J.W., Bilen, M.A., Cardenas, M., Wilkinson, S., Lake, R., Sowalsky, A.G., et al. (2019). An intra-tumoral niche maintains and differentiates stem-like CD8 T cells. Nature *576*, 465–470. https://doi.org/10.1038/s41586-019-1836-5.

82. Gonzalez-Cao, M., Martinez-Picado, J., Karachaliou, N., Rosell, R., and Meyerhans, A. (2019). Cancer immunotherapy of patients with HIV infection. Clin. Transl. Oncol. *21*, 713–720. https://doi.org/10.1007/s12094-018-1981-6.

83. Gardiner, D., Lalezari, J., Lawitz, E., DiMicco, M., Ghalib, R., Reddy, K.R., Chang, K.-M., Sulkowski, M., Marro, S.O., Anderson, J., et al. (2013). A randomized, double-blind, placebo-controlled assessment of BMS-936558, a fully human monoclonal antibody to programmed death-1 (PD-1), in patients with chronic hepatitis C virus infection. PLoS One *8*, e63818. https://doi.org/10.1371/journal.pone.0063818.

84. El-Khoueiry, A.B., Sangro, B., Yau, T., Crocenzi, T.S., Kudo, M., Hsu, C., Kim, T.-Y., Choo, S.-P., Trojan, J., Welling, T.H., et al. (2017). Nivolumab in patients with advanced hepatocellular carcinoma (CheckMate 040): an open-label, non-comparative, phase 1/2 dose escalation and expansion trial. Lancet *389*, 2492–2502. https://doi.org/10.1016/S0140-6736(17)31046-2.

85. Peligero, C., Argilaguet, J., Güerri-Fernandez, R., Torres, B., Ligero, C., Colomer, P., Plana, M., Knobel, H., García, F., and Meyerhans, A. (2015). PD-L1 blockade differentially impacts regulatory T cells from HIV-infected individuals depending on plasma viremia. PLoS Pathog. *11*, e1005270. https://doi.org/10.1371/journal.ppat.1005270.

86. Bailón, L., Llano, A., Cedeño, S., Escribà, T., Rosás-Umbert, M., Parera, M., Casadellà, M., Lopez, M., Pérez, F., Oriol-Tordera, B., et al. (2022). Safety, immunogenicity and effect on viral rebound of HTI vaccines in early treated HIV-1 infection: a randomized, placebo-controlled phase 1 trial. Nat. Med. *28*, 2611–2621. https://doi.org/10.1038/s41591-022-02060-2.

87. Gudjonsson, A., Lysén, A., Balan, S., Sundvold-Gjerstad, V., Arnold-Schrauf, C., Richter, L., Bækkevold, E.S., Dalod, M., Bogen, B., and Fossum, E. (2017). Targeting influenza virus hemagglutinin to Xcr1 dendritic cells in the absence of receptor-mediated endocytosis enhances protective antibody responses. J. Immunol. *198*, 2785–2795. https://doi.org/10.4049/jimmunol.1601881.

88. Battegay, M., Cooper, S., Althage, A., Bänziger, J., Hengartner, H., and Zinkernagel, R.M. (1991). Quantification of lymphocytic choriomeningitis virus with an immunological focus assay in 24- or 96-well plates. J. Virol. Methods *33*, 191–198. https://doi.org/10.1016/0166-0934(91)90018-u.

89. Fredriksen, A.B., Sandlie, I., and Bogen, B. (2006). DNA vaccines increase immunogenicity of idiotypic tumor antigen by targeting novel fusion proteins to antigen-presenting cells. Mol. Ther. *13*, 776–785. https://doi.org/10.1016/j.ymthe.2005.10.019.

90. Grødeland, G., Mjaaland, S., Tunheim, G., Fredriksen, A.B., and Bogen, B. (2013). The specificity of targeted vaccines for APC surface molecules influences the immune response phenotype. PLoS One *8*, e80008. https://doi.org/10.1371/journal.pone.0080008.

## STAR★METHODS

### KEY RESOURCES TABLE

| REAGENT or RESOURCE | SOURCE | IDENTIFIER |
|---|---|---|
| Antibodies | | |
| Alexa Fluor® 647 Rat Anti-Mouse I-A/I-E (clone M5/114) | BD Biosciences | Cat#562367; RRID:AB_11152078 |
| Alexa Fluor® 647 anti-mouse CXCL9 (MIG) (clone MIG-2F5.5) | BioLegend | Cat#515606; RRID:AB_1877135 |
| Alexa Fluor® 700 anti-mouse CD107a (LAMP-1) (clone 1D4B) | BioLegend | Cat#121627; RRID:AB_2783062 |
| Anti-LCMV nucleoprotein (clone VL-4) | BioXcell | Cat#BE0106; RRID:AB_10949017 |
| Anti-mouse XCL1/Lymphotactin (clone 80222) | R&Dsytems | Cat#MAB486; RRID:AB_2216913 |
| APC Hamster Anti-Mouse CD3e (clone 145-2C11) | BD Biosciences | Cat#553066; RRID:AB_398529 |
| APC Rat anti-Mouse CD172a (SIRPα) (clone P84) | BD Biosciences | Cat#560106; RRID:AB_1645218 |
| APC anti-mouse CD366 (Tim3) (clone RMT3-23) | Miltenyi | Cat#130-102-366; RRID:AB_2654180 |
| APC/Fire™ 750 anti-mouse CD40 (clone 3/23) | BioLegend | Cat#124631; RRID:AB_2734193 |
| APC/Cyanine7 anti-mouse MHC Class II (I-A/I-E) (clone M5/114.15.2) | BioLegend | Cat#107627; RRID:AB_1659252 |
| BV421 Rat Anti-Mouse CD44 (clone IM7) | BD Biosciences | Cat#563970; RRID:AB_2738517 |
| BV421 Rat Anti-Mouse CD107b (clone ABL-93) | BD Biosciences | Cat#564249; RRID:AB_2738702 |
| Brilliant Violet 421™ anti-mouse Ki-67 (clone 16A8) | BD Biosciences | Cat#652411; RRID:AB_2562663 |
| Brilliant Violet 421™ anti-mouse/rat XCR1 (clone ZET) | BioLegend | Cat#148216; RRID:AB_2565230 |
| Brilliant Violet 510 anti-mouse/rat XCR1 (clone ZET) | BioLegend | Cat#148218; RRID:AB_2565231 |
| BV605 Hamster Anti-Mouse CD279 (clone J43) | BD Biosciences | Cat#563059; RRID:AB_2737980 |
| BV711 Hamster Anti-Mouse CD80 (clone 16-10A1) | BD Biosciences | Cat#740698; RRID:AB_2740382 |
| Brilliant Violet 785™ anti-mouse CD3 (clone 17A2) | BioLegend | Cat#100231; RRID:AB_11218805 |
| eFluor 450 anti-mouse CD44 (clone IM7) | Thermo Fisher | Cat#48-0441-80; RRID:AB_1272250 |
| FITC anti-mouse CD44 (clone IM7) | Thermo Fisher | Cat#11-0441-82; RRID:AB_465045 |
| FITC Rat Anti-Mouse CD86 (clone GL1) | BD Biosciences | Cat#553691; RRID:AB_394993 |
| FITC anti-mouse CD279 (PD-1) (clone J43) | Thermo Fisher | Cat#11-9985-81; RRID:AB_465471 |
| FITC Rat Anti-Mouse IFN-γ (clone XMG1.2) | BD Biosciences | Cat#554411; RRID:AB_395375 |
| FITC anti-mouse MHC Class II (I-A/I-E) (clone M5/114.15.2) | Thermo Fisher | Cat#11-5321-81; RRID:AB_465231 |
| InVivoMAb anti-mouse PD-L1 (B7-H1) | BioXcell | Cat#BE0101; RRID:AB_10949073 |
| InVivoMAb anti-mouse CXCL9 (MIG) (clone MIG-2F5.5) | BioXcell | Cat#BE0309; RRID:AB_2736989 |
| InVivoMAb anti-mouse IL-12 p40 (clone C17.8) | BioXcell | Cat#BE0051; RRID:AB_1107698 |
| Pacific Blue anti-mouse CD3 (clone 17A2) | BioLegend | Cat#100213; RRID:AB_493644 |
| Pacific Blue anti-mouse CD19 (clone 6D5) | BioLegend | Cat#115526; RRID:AB_493341 |
| Pacific Blue anti-mouse Nk1.1 (clone PK136) | BioLegend | Cat#108721; RRID:AB_2234352 |
| Peroxidase AffiniPure Goat Anti-Rat IgG (H + L) | Jackson ImmunoResearch | Cat#112-035-003; RRID:AB_2338128 |
| PE Rat Anti-Mouse CD4 (clone H129.19) | BD Biosciences | Cat#553653; RRID:AB_394973 |
| PE anti-mouse CD172a (SIRPα) (clone P84) | BioLegend | Cat#144011; RRID:AB_2563549 |
| PE anti-mouse CD274 (B7-H1, PD-L1) (clone 10F.9G2) | BioLegend | Cat#124307; RRID:AB_2073557 |
| PE anti-mouse IL-12/IL-23 p40 (clone C17.8) | Thermo Fisher | Cat#12-7123-81; RRID:AB_466184 |
| PE anti-mouse SiglecH (clone eBio440c) | Thermo Fisher | Cat#12-0333-82; RRID:AB_10597139 |
| PE TNF alpha (clone MP6-XT22) | Thermo Fisher | Cat#12-7321-41; RRID:AB_10854722 |
| PerCP-Cy™5.5 Rat Anti-Mouse CD4 (clone RM4-5) | BD Biosciences | Cat#550954; RRID:AB_393977 |
| PerCP-Cy™5.5 Rat Anti-Mouse CD8a (clone 53–6.7) | BD Biosciences | Cat#551162; RRID:AB_394081 |
| PerCP-Cy5.5 Hamster Anti-Mouse CD11c (clone HL3) | BD Biosciences | Cat#560584; RRID:AB_1727422 |
| PE-CF594 Rat Anti-Mouse CD45R (clone RA3-6B2) | BD Biosciences | Cat#562313; RRID:AB_11154399 |
| PE/Dazzle™ 594 anti-mouse CD185 (CXCR5) (clone L138D7) | BioLegend | Cat#145521; RRID:AB_2563643 |
| PE-Cy5 anti-mouse CD40 (clone 3/23) | BioLegend | Cat#124617; RRID:AB_2075923 |

(*Continued on next page*)

*Continued*

| REAGENT or RESOURCE | SOURCE | IDENTIFIER |
|---|---|---|
| PE-Cy™7 Hamster Anti-Mouse CD3e (clone 145-2C11) | BD Biosciences | Cat#561100; RRID:AB_10562036 |
| PE-Cy™7 Rat Anti-Mouse CD8a (clone 53–6.7) | BD Biosciences | Cat#552877; RRID:AB_394506 |
| PE-Cy7 anti-mouse CD69 (clone H1.2F3) | Thermo Fisher | Cat#25-0691-82; RRID:AB_469637 |
| PE-Cy7 CD86 (B7-2) (clone GL1), | Thermo Fisher | Cat#25-0862-80; RRID:AB_2573371 |
| PE-Cy7 anti-mouse CD366 (Tim3) (clone RMT3-23) | Thermo Fisher | Cat#25-5870-82; RRID:AB_2573483 |
| Purified Rat anti-mouse CD16/32 (Mouse BD Fc Block™) (clone 2.4G2) | BD Biosciences | Cat#553141; RRID:AB_394656 |
| **Bacterial and virus strains** | | |
| LCMV Docile | LCMV Docile | Grew in house |
| E. coli DH5alpha | E. coli DH5alpha | Cat#C2987H |
| **Chemicals, peptides, and recombinant proteins** | | |
| Diphtheria Toxin from Corynebacterium diphtheriae | Sigma | Cat#D0564 |
| TransIT™-QR Delivery Solution | Mirus | Cat#MIR5240 |
| Alexa Fluor™ 488 Antibody Labeling Kit | ThermoFisher | Cat#A20181 |
| LIVE/DEAD™ Fixable Violet Dead Cell Stain Kit | ThermoFisher | Cat#L34955 |
| BD Horizon™ Fixable Viability Stain 780 | BD Biosciences | Cat#565388 |
| Zombie NIR™ Fixable Viability Kit | BioLegend | Cat#423105 |
| GP33 Biotinylated Monomer - H-2 Db LCMV (KAVYNFATC) | MBL International | Cat#TB-5002-M |
| Streptavidin PE Conjugate | Thermo Fisher | Cat#12-4317-87 |
| DNase I recombinant, RNase-free | Roche | Cat#4716728001 |
| Liberase™ DL Research Grade | Roche | Cat#5401160001 |
| Brefeldin A | Sigma | Cat#B7651 |
| GP(33–41) peptide KAVYNFATM | David Andreu | Custom |
| NP(396–404) peptide FQPQNGQFI | David Andreu | Custom |
| Ampicillin 100 mg/mL, 0.2 μm filtered | Sigma | Cat#A5354 |
| Luria Broth | ThermoFisher | Cat#12795027 |
| **Critical commercial assays** | | |
| DAB Substrate Kit, Peroxidase (HRP), with Nickel | Vector Laboratories | Cat#SK-4100 |
| NucleoBond Xtra Maxi EF Kit | Macherey-Nagel GmbH & Co | Cat# 740424.10 |
| QIAGEN EndoFree MegaPrep Kit | QIAGEN | Cat#12381 |
| Pan Dendritic Cell Isolation Kit (mouse) | Miltenyi Biotec | Cat#130-100-875 |
| **Experimental models: Cell lines** | | |
| MC57 cell line | Grown in house | N/A |
| L929 cell line | Grown in house | N/A |
| VL-4 hybridoma | Grown in house | N/A |
| **Experimental models: Organisms/strains** | | |
| C57BL/6J mice | NCI/Charles River | Cat#027; RRID:IMSR_JAX:000664 |
| XCR1DTRVenus mice | Yamazaki et al.[56] | Bred in house |
| **Recombinant DNA** | | |
| pEF-BOS-bsr vector | Iwabuchi et al.[54] | N/A |
| pEF-BOS-humanFlt3L-bsr vector | Iwabuchi et al.[54] | N/A |
| XCL1-HA fusion vaccine | Fossum et al.[58] | N/A |
| XCL1-LCMV-NP fusion vaccine | Even Fossum | N/A |
| αNIP-LCMV-NP fusion vaccine | Even Fossum | N/A |
| **Software and algorithms** | | |
| FlowJo v10.7.1 | TreeStar | https://www.flowjo.com/solutions/flowjo/downloads |

(*Continued on next page*)

*Continued*

| REAGENT or RESOURCE | SOURCE | IDENTIFIER |
|---|---|---|
| GraphPad Prism v9 | GraphPad Software | https://www.graphpad.com/scientificsoftware/prism/ |
| Other | | |
| RPMI-1640 medium | ThermoFisher | Cat#21875-034 |
| DMEM, high glucose, pyruvate | ThermoFisher | Cat#41966-052 |
| IMDM, Hepes medium | ThermoFisher | Cat#21980-032 |
| Fetal Bovine Serum | Sigma | Cat#F7524 |
| Penicillin-Streptomycin | ThermoFisher | Cat#15140122 |
| β-mercaptoethanol | Sigma | Cat#M3148 |
| Sodium pyruvate | Sigma | Cat#S8636 |
| Trypsin-EDTA 0.25% | ThermoFisher | Cat#25200 |
| DMSO | Sigma | Cat#D4540 |

## RESOURCE AVAILABILITY

### Lead contact

Further information and requests for resources and reagents should be directed to the lead contact, Andreas Meyerhans (andreas.meyerhans@upf.edu).

### Materials availability

This study did not generate new unique reagents.

### Data and code availability

- All data reported in this paper will be shared by the lead contact upon request.
- This paper does not report original code.
- Any additional information required to reanalyze the data reported in this paper is available from the lead contact upon request.

## EXPERIMENTAL MODEL AND SUBJECT DETAILS

### Mice

Male C57BL/6J mice (RRID:IMSR_JAX:000664) aged 6 weeks were purchased from Charles River Laboratories and XCR1-DTRvenus mice were obtained from Dr. Tsuneyasu Kaisho,[56] bred and maintained under specific pathogen-free conditions at in-house facilities. Male and female XCR1-DTRvenus mice aged 6–12 weeks were used for experimentation. The number of animals for each experiment was determined based on previous experience with the model system. All animal work was conducted according to the guidelines from Generalitat de Catalunya approved by the ethical committees for animal experimentation at Parc de Recerca Biomèdica de Barcelona (CEEA-PRBB, Spain).

### Viruses and infections

LCMV Docile ($LCMV_{Doc}$) was grown in L929 cells and titrated using focus forming assay on MC57 cells.[88] Mice were infected intraperitoneally with either a low-dose ($2 \times 10^2$ plaque-forming units) or a high dose ($2 \times 10^6$ plaque-forming units) of $LCMV_{Doc}$ to induce an acute or chronic infection, respectively.

## METHOD DETAILS

### Cell preparation, flow cytometry and cell sorting

Spleens were mechanically disrupted onto a 40μM cell strainer using the plunger of a 1mL syringe and incubated in 5mL of 0.15M Ammonium chloride buffer for 5 min at room temperature (RT) for red blood cell lysis. Cell suspensions were washed in RPMI (GIBCO) supplemented with 10% FBS, 1% penn/strep, 0.05mM β-Mercaptoethanol and 1mM Sodium Pyruvate (cRPMI). For LCMV-NP + DC marker analysis, spleens were enzymatically digested at 37°C for 30 min with a mix of 0.2 mg/ml DNAse and 0.16 mg/ml Liberase and DC were enriched using the Pan-Dendritic Cell Isolation kit (Miltenyi).

For flow cytometric analysis, equal number of cells were stained with Live/Dead Fixable Violet Cell Stain (ThermoFisher Scientific) or Fixable Viability Stain 780 (BD Biosciences) in PBS for 15 min at RT followed by staining with extracellular antibodies for 20 min on ice in FACS buffer (PBS 5% FCS, 0.5% BSA, 0.07% $NaN_3$). Biotinylated MHC class I monomer (MBL International) was tetramerized by addition of PE-conjugated Streptavidin over 10-time intervals and added together with extracellular antibodies. Cells were then fixed for 20 min on ice with 2% Formaldehyde and stained with antibodies for intracellular proteins (XCL1, LCMV-NP, IFN$\gamma$, IL-12(p40), CXCL-9, Ki67) for 20 min on ice in Perm/Wash buffer (PBS 1% FCS, $NaN_3$ 0.1%, Saponin 0.1%). All antibodies were purchased from either BD Biosciences, eBioscience, BioLegend, Miltenyi or R&D Systems. Samples were acquired on an LSR Fortessa (BD Biosciences), a SP6800 Spectral (Sony) or an Aurora (Cytek) analyzer. FACS data was analyzed using FlowJo 10 software (Tree Star Inc).

### Intracellular cytokine staining

For determination of cytokine-producing T cells, splenocytes (1–2x$10^6$) were stimulated with $GP_{33-41}$(1 μg/mL) or $NP_{396-404}$ (1 μg/mL) peptides for 5h at 37C 5% $CO_2$ in cRPMI in the presence of Brefeldin A (BFA, Sigma) before antibody staining. Conjugated antibodies to the granular membrane proteins CD107a and CD107b were added to the cells prior to stimulation. For determination of XCL1-producing T cells, Ki67 + T cells and IL-12(p40) and CXCL-9-producing dendritic cells, spleens were harvested in media containing BFA and antibody staining was performed without additional stimulation.

### Virus load quantification

Viral titers from spleens of infected mice were quantified by focus forming assay on MC57 cells as described previously.[88] Briefly, spleens were frozen at −80°C right after collection. Tissue was mechanically disrupted and 500μL of RPMI 2% FBS were added to the homogenization. One in ten-fold dilutions were prepared and overlaid onto MC57 cell monolayers in 24-well plates. After 48h of incubation at 37C 5% $CO_2$, staining was performed using monoclonal rat anti-LCMV antibody (VL-4) for 1h, Peroxidase Anti-Rat IgG Polyclonal Ab (Jackson ImmunoResearch) and DAB Peroxidase substrate kit (Vector Laboratories).

### *In vivo* anti-PD-L1 antibody treatment

Where indicated, groups of mice were injected with 200μg of anti-PD-L1-specific mAb (10F.9G2, BioXCell) intraperitoneally three times, every third day starting at the indicated time points. As a control, physiological serum was administered.

### *In vivo* cell depletion

For depletion of XCR1+ dendritic cells, groups of heterozygote XCR1-DTRvenus mice were injected with 25 ng/g body weight of Diphtheria Toxin (DT) intraperitoneally three times, every third day starting at the indicated time points. As control, physiological serum was administered.

### *In vivo* transfection of human Flt3L

Human Flt3L (GenBank: NM_001459.3) gene was previously subcloned into the pEF-BOS-bsr plasmid.54 Plasmid DNA was transformed into *E. coli DH5α* (New England Biolabs) and purified using the NucleoBond Xtra Maxi EF Kit (Macherey-Nagel GmbH & Co). For hydrodynamic gene delivery, 50μg plasmid DNA was diluted in 2mL TransIT-QR Hydrodynamic Delivery Solution (Mirus Bio LLC) and rapidly injected intravenously (tail vein) in 3-5s using a 27-gauge needle. As control, 50μg of the empty vector pEF-BOS-bsr plasmid was administered.

### *In vivo* neutralization of CXCL-9 and IL-12

Where indicated, groups of mice were injected intraperitoneally with 300μg of anti-CXCL-9-specific mAb (MIG-2F5.5, BioXCell) four times, every other day or with 500μg anti-IL-12-specific mAb (C17.8, BioXCell) daily, starting at the indicated time points. As a control, physiological serum was administered.

### Electroporation of Xcl1-targeted fusion vaccines

The fusion vaccines are dimeric molecules where each monomer consists of a targeting unit, an antigenic unit, and a dimerization unit.[89] Construction of the XCL1-targeted fusion vaccines has been described previously.[58,90] Nucleotide sequences encoding the LCMV nucleoprotein were obtained from GenScript, with added 5′ BsmI and 3′ BsiWI sites and cloned into the vaccine construct. Fusion vaccines containing a single chain variable fragment specific to the hapten (5-iodo-4-hydroxy-3- nitrophenylacetyl) NIP were used as non-targeted controls and vaccines expressing the Influenza virus hemagglutinin as negative controls. All plasmids were transformed into *E. coli DH5α* (New England Biolabs) and purified using the QIAGEN Endofree MegaPrep Kit according to the manufacturer's instructions. The indicated groups of mice were anesthetized with isoflurane and after shaving the lower back, 25μL of DNA vaccine (0.5 μg/μL in physiological serum) was injected intradermally on the left flank followed by electroporation using the ECM 830 Electroporation System (BTX Molecular Delivery Systems) with 2 pulses of 450 V/cm × 2.5μs and 8 pulses of 110 V/cm × 10ms. The procedure was repeated on the right flank.

## QUANTIFICATION AND STATISTICAL ANALYSIS

Graphs were compiled and statistical analyses were performed with Prism software (GraphPad). Statistical significance was evaluated with the unpaired t test when comparing two groups and one-way ANOVA when comparing more than two groups. Non-significant differences were indicated as "ns". p-values below 0.05 were considered significant and were indicated by asterisks: *$p < 0.05$; **$p < 0.01$; ***$p < 0.001$; ****$p < 0.0001$.

**Cell Reports, Volume *42***

## Supplemental information

# XCR1+ DCs are critical for T cell-mediated immunotherapy of chronic viral infections

**Eva Domenjo-Vila, Valentina Casella, Ryutaro Iwabuchi, Even Fossum, Mireia Pedragosa, Quim Castellví, Paula Cebollada Rica, Tsuneyasu Kaisho, Kazutaka Terahara, Gennady Bocharov, Jordi Argilaguet, and Andreas Meyerhans**

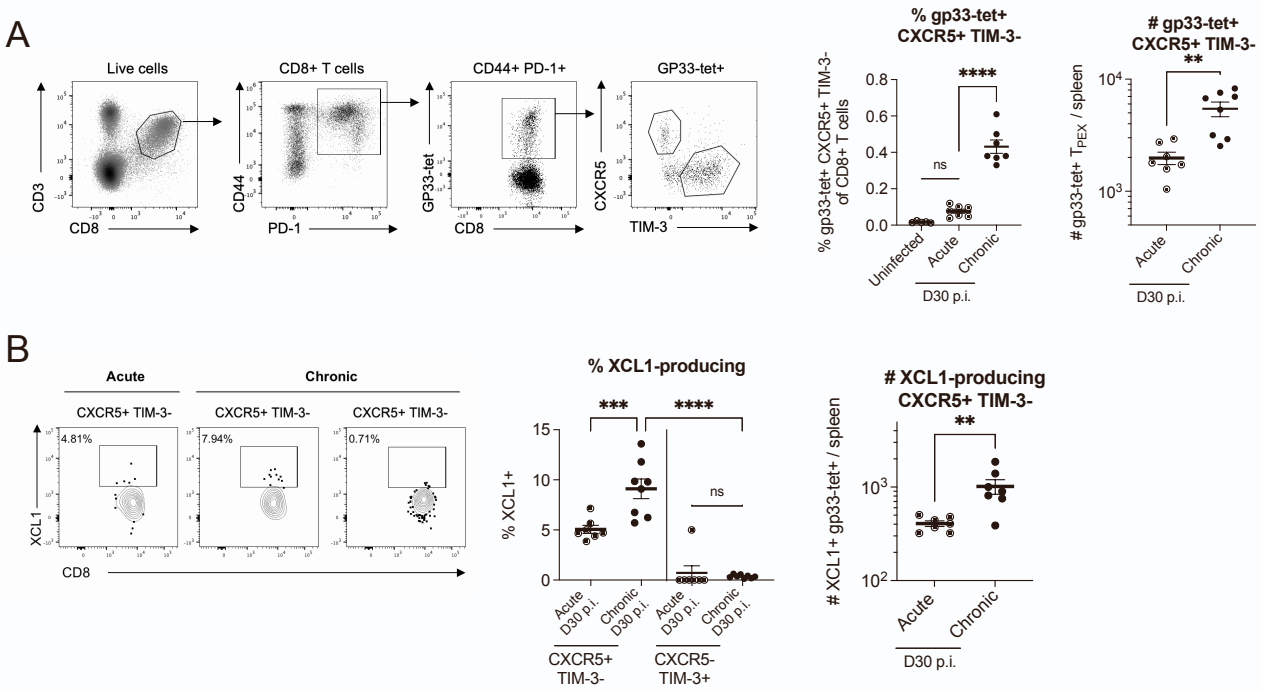


**Figure S1. Increased gp33-specific TPEX numbers and XCL1 production in chronic LCMV infection (related to Figure 1).**

Mice were chronically infected with a high-dose of LCMV strain Docile (LCMVDoc), acutely infected with a low-dose of LCMV or left uninfected, and splenic gp33-specific CD8+ T cells were analyzed by flow cytometry.

(A) Representative gating of gp33-tet+ CXCR5+ TIM-3- and quantification from splenocytes isolated from LCMV-infected C57BL6/J mouse at day 30 p.i..

(B) Representative plots and quantification of XCL1 production by gp33-tet+ TPEX and TEX.

Data shown are the mean ± SEM from 6 mice per group. Statistical analysis was performed using unpaired t-test or one-way ANOVA with Tukey's multiple comparisons (ns = not significant; *p < 0.05; **p < 0.01; ***p < 0.001; ****p < 0.0001).

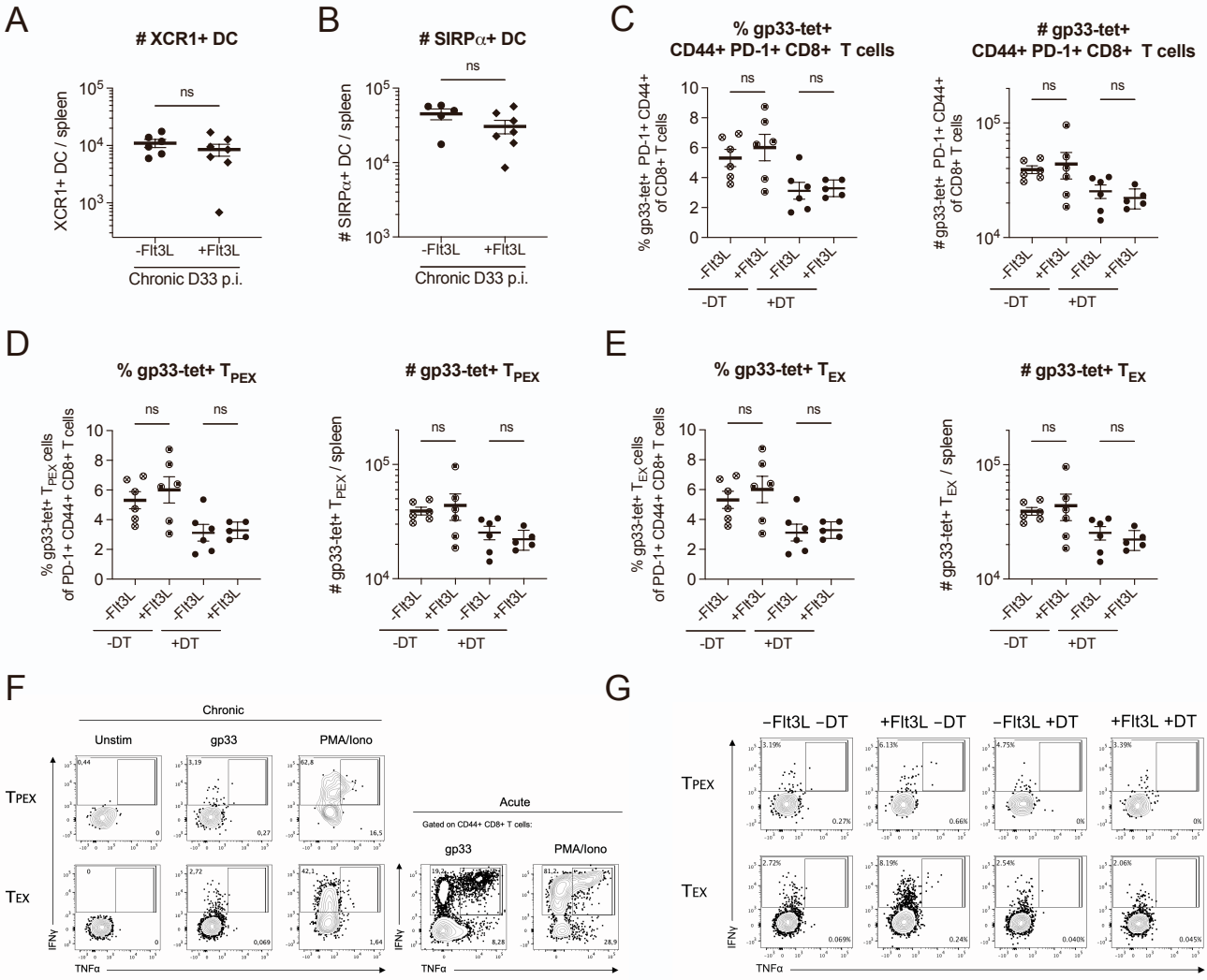


**Figure S2. Quantification of DC and gp33-specific exhausted CD8+ T cell subsets 12 days after Flt3L *in vivo* transfection (related to Figure 2).**

Chronic LCMV-infected mice were transfected with empty vector pEF-BOS-bsr plasmid (-Flt3L) or pEF-BOS-Flt3L-bsr plasmid (+Flt3L), and treated with Diphtheria Toxin (+DT) or left untreated.

(A-E) Absolute numbers of XCR1+ (A) and SIRPα+ (B) DC, and gp33-tet+ PD-1+ CD44+ CD8+ T cells (C), TPEX (D) and TEX (E) at day 33 p.i. (12 days after Flt3L *in vivo* transfection).

(F and G) Representative plots showing stimulation controls (F) and GP33-41-specific IFNγ-producing and IFNγ-producing and TNFα-producing (G) TPEX and TEX.

Data shown are the mean ± SEM from 6 mice per group. Statistical analysis was performed using one-way ANOVA with Tukey's multiple comparisons (ns = not significant).

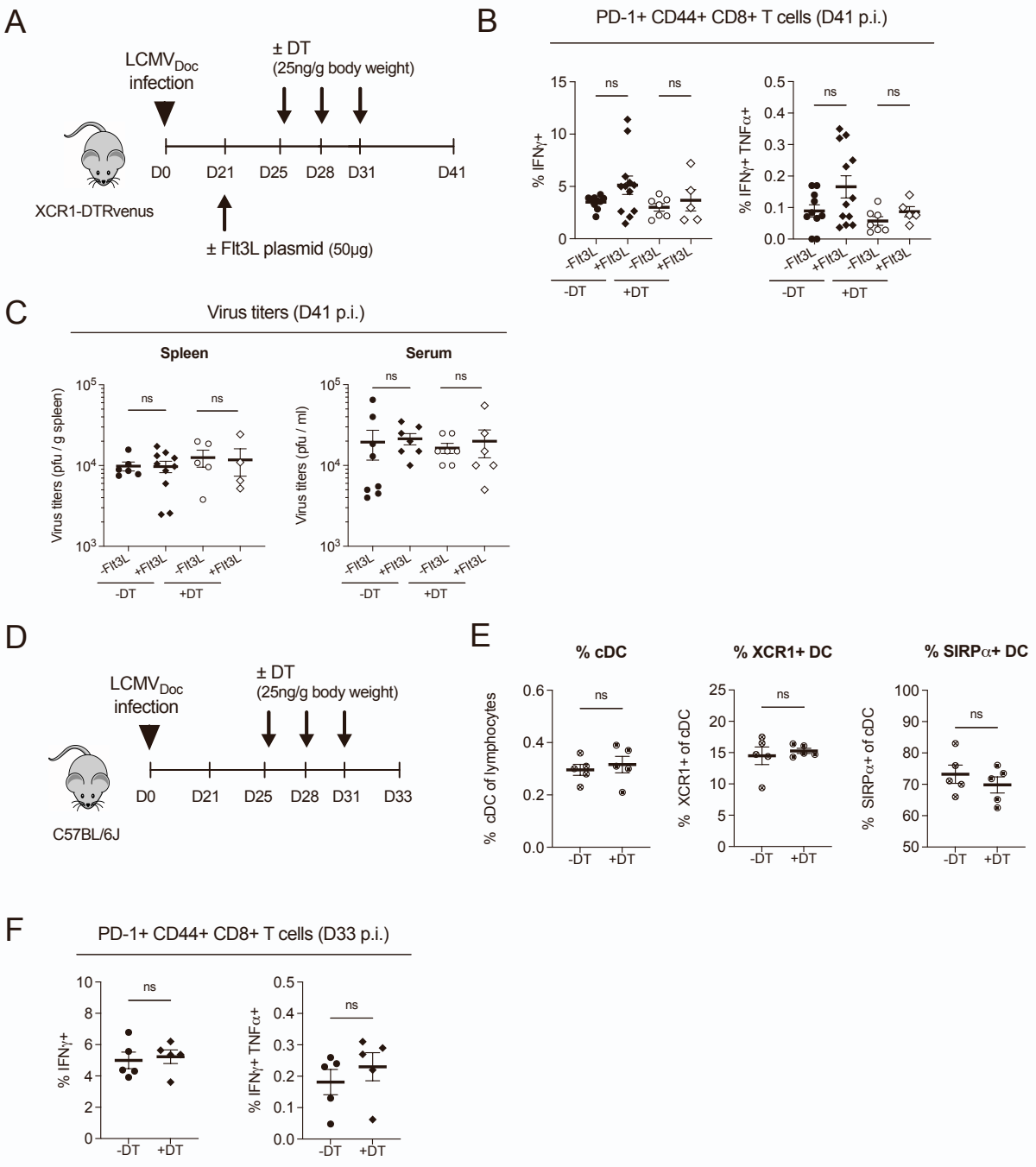


**Figure S3. XCR1+ DC expansion transitorily enhances antiviral CD8+ T cell immunity in chronic infections (related to Figure 2).**

(A) Schematic representation of Flt3L and DT treatment regimens in XCR1-DTRvenus mice.

(B and C) At day 41 p.i., IFNγ-producing and IFNγ- plus TNFα-producing PD-1+ CD44+ CD8+ T cells (B) and virus loads in spleen and serum (C) were analyzed.

(D) Chronic LCMV-infected wild-type mice were treated with Diphtheria Toxin (+DT) or left untreated as shown in the schematic representation.

(E and F) Frequencies of XCR1+ and SIRPα+ DC (E) and IFNγ-producing and TNFα-producing PD-1+ CD44+ CD8+ T cells (F) at day 33 p.i. are shown.

Data shown are the mean ± SEM from 5-12 mice per group. Statistical analysis was performed using one-way ANOVA with Tukey's multiple comparisons (ns = not significant).

A

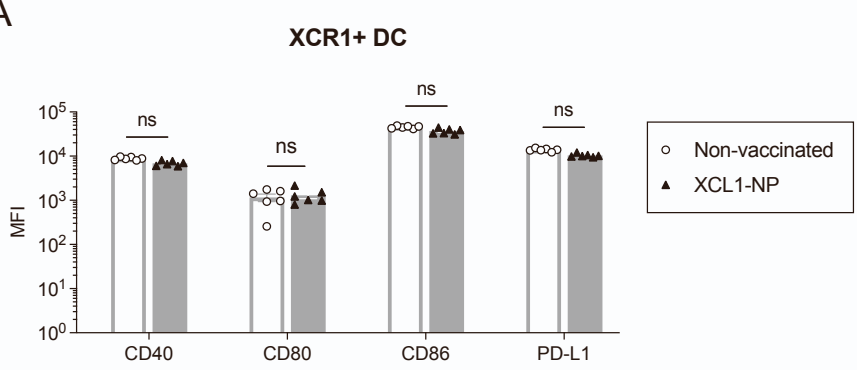


**Figure S4. Phenotypic characterization of XCR1+ and SIRPα+ DC after vaccination of XCL1-NP during chronic infection (related to Figure 2).**

(A) Chronic LCMV-infected mice were vaccinated with XCL1-NP at day 28 p.i. or left unvaccinated, and sacrificed at day 30 p.i.. MFI of CD40, CD80, CD86 and PD-L1 proteins expressed by LCMV-NP+ XCR1+ and SIRPα+ DC are shown. Data shown are the mean ± SEM from 6 mice per group. Statistical analysis was performed using unpaired t-test (ns = not significant).

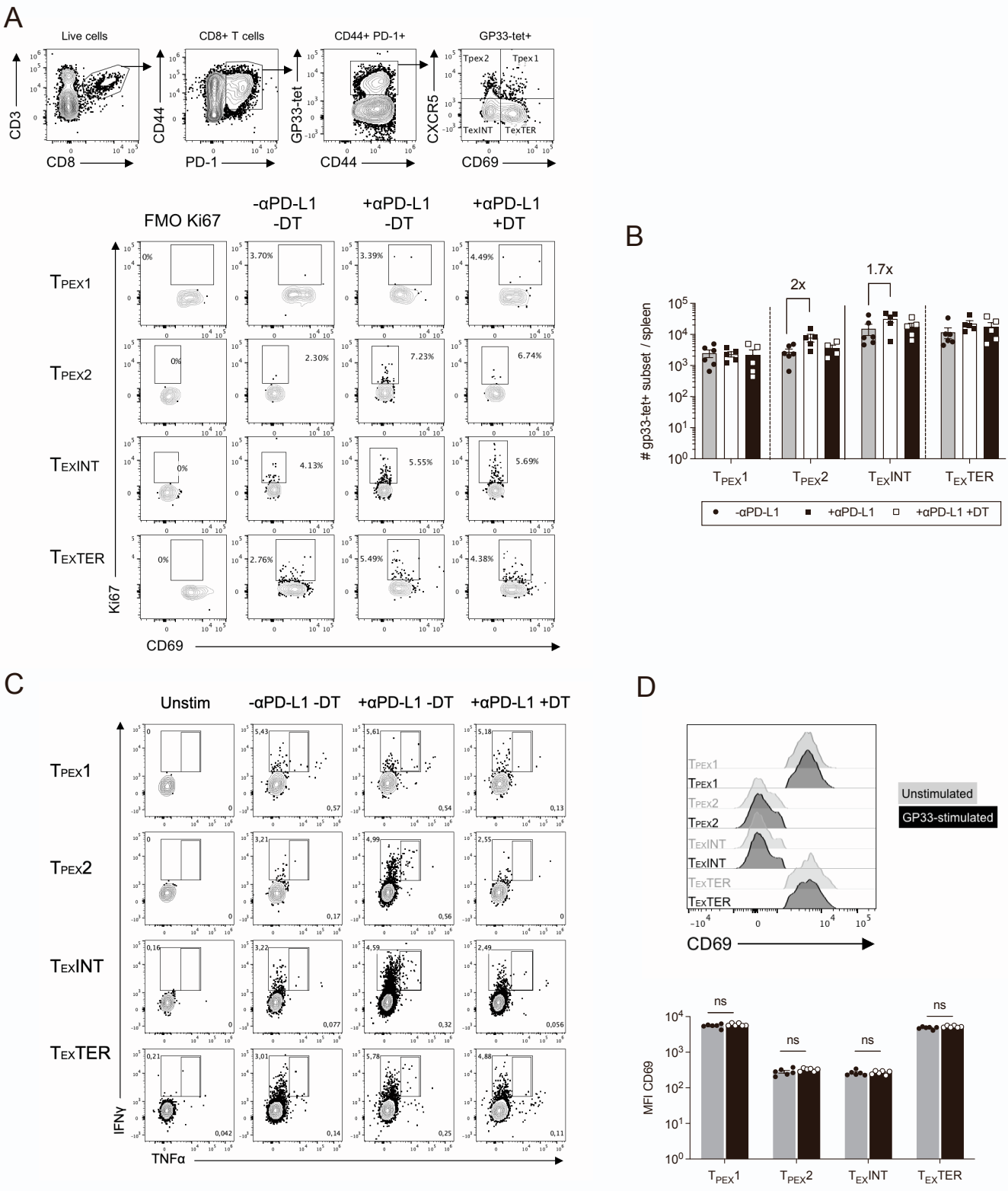


**Figure S5. Functional changes of exhausted CD8+ T cells upon anti-PD-L1 treatment in the presence or absence of XCR1+ DC (related to Figure 4).**

Chronic LCMV-infected mice were treated with anti-PD-L1 antibodies in the presence or absence (+DT) of XCR1+ DC, and sacrificed at day 30 p.i..

(A and B) Representative gating strategy and dot plots of proliferating Ki67+ (A) and absolute number quantification of exhausted CD8+ T cell subsets. Fold change over untreated (αPD-L1−) group (n = 5 mice).

(C) Representative dot plots of $GP_{33-41}$-specific IFNγ-producing exhausted CD8+ T cell subsets.

(D) Representative histograms and MFI quantification of CD69 expression on TPEX1, TPEX2, TEXINT and TEXTER analyzed in unstimulated versus gp33-peptide stimulated matched samples. Data shown are the mean ± SEM from 6 mice per group. Statistical analysis was performed using t-test (ns = not significant).

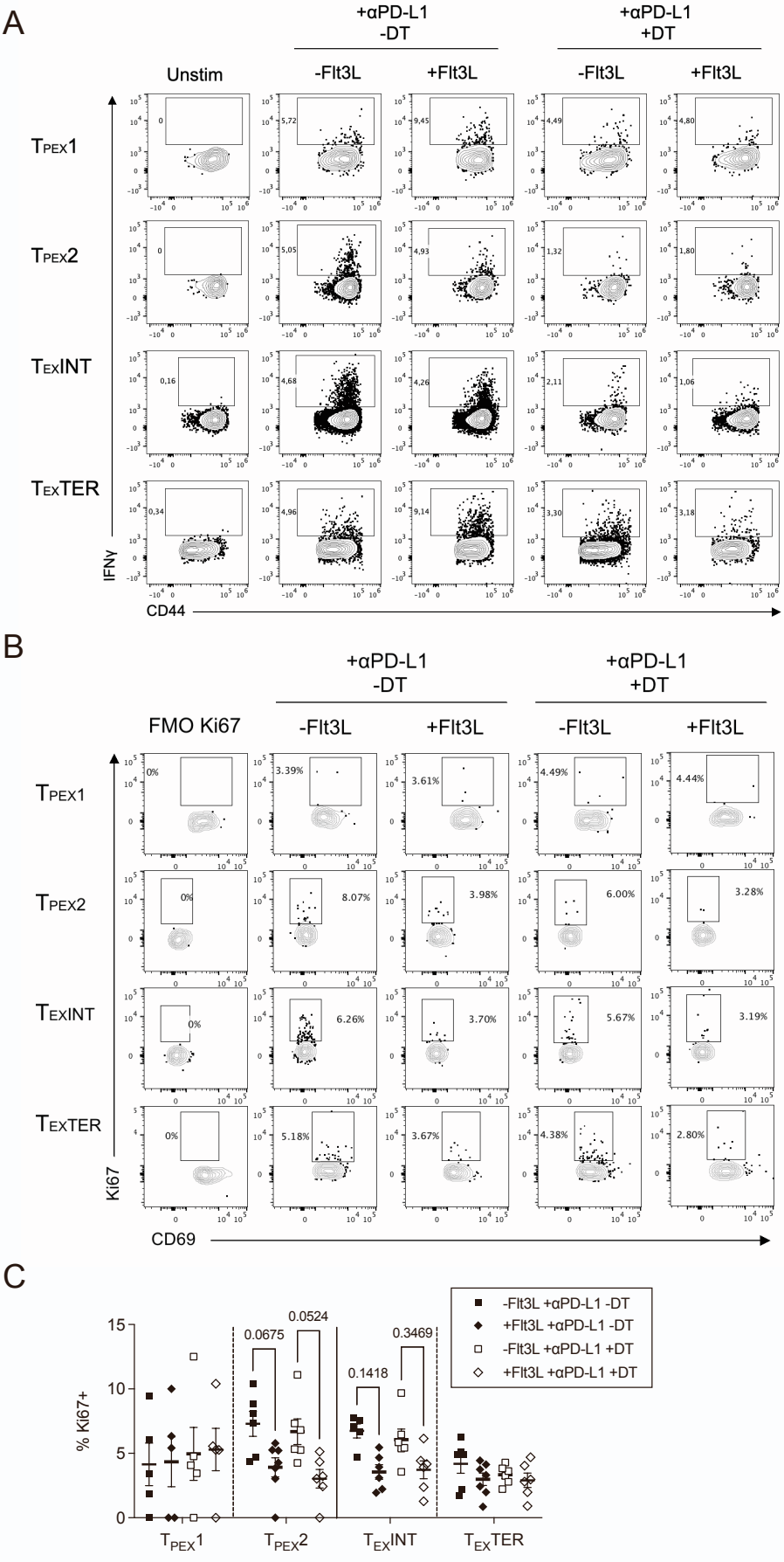


**Figure S6. Combination of anti-PD-L1 treatment with Flt3L-mediated expansion of DC (related to Figure 6).**

Chronic LCMV-infected and anti-PD-L1 treated mice were transfected with Flt3L-expressing plasmid (+Flt3L) in the presence or absence (+DT) of XCR1+ DC, and sacrificed at day 33 p.i..

(A-C) Representative dot plots of GP33-41-specific IFNγ-producing (A) and proliferating Ki67+ (B) exhausted CD8+ T cell subsets. (C) Percentages of Ki-67+ TPEX1, TPEX2, TEXINT and TEXTER are shown.